Long-Range Forecasting and Climate Research

Numerical Models of the Raingauge Exposure Problem

Field Experiments and an Improved Collector Design

by

C. K. Folland

Revised Paper

LRFC 19

May 1988

JM

REVISED PAPER

NUMERICAL MODELS OF THE RAINGAUGE EXPOSURE PROBLEM, FIELD EXPERIMENTS AND AN IMPROVED COLLECTOR DESIGN

C.K. FOLLAND

Meteorological Office, Bracknell, Berks, UK, RG12 2SZ

April 1988

For Q.J.Roy. Met.Soc.

LONDON, METEOROLOGICAL OFFICE.
Long-Range Forecasting and Climate Research
Memorandum No.19

Numerical models of the raingauge exposure problem field experiments, and an improved collector design. Revised paper.

07560688 FH1B

NUMERICAL MODELS OF THE RAINGAUGE EXPOSURE PROBLEM, FIELD EXPERIMENTS, AND AN IMPROVED COLLECTOR DESIGN

C K Folland

Meteorological Office, Bracknell, Berks. UK

ABSTRACT

A new design of conventional raingauge collector is proposed that minimises the most important source of systematic error in point rainfall measurements, that due to the interaction of the ambient wind field with the gauge itself (the "raingauge exposure" problem). Basic physical principles, numerical simulations and extensive field trials in England and Denmark are also used to provide a consistent quantitative description of the wind-induced errors of conventional cylindrical gauges.

It is shown that an inverted conical collector with a large semi-vertical angle may provide the basis of an adequate solution of the raingauge exposure problem. The need to minimise outsplash demands that the collector should have a fairly large diameter and take the form of a flat champagne glass. A small diameter flat champagne glass collector has been tested for over $3^1/_2$ years against a standard 5" cylindrical gauge, a 5" pit gauge and an inverted conical gauge at the Institute of Hydrology, Wallingford, UK. The insensitivity of the losses of the "flat champagne glass"-shaped collector to wind speed at low rates of rainfall is confirmed, as well as the need for a larger collector diameter to minimise outsplash. A combination of a "steep champagne glass" gauge and a "flat

champagne glass" gauge might lead to even better estimates of rainfall in high winds, notably on ships, and could provide a low-cost approach to improving snowfall measurements on land.

1. INTRODUCTION

The precipitation catch from conventional cylindrical raingauges can suffer from large systematic errors when high winds blow past the entrance to the gauge, if, as is usual, the entrance is placed some distance above the ground (usually 30 cm in UK, though 150 cm is common in Europe). Rodda (1968) gives a detailed discussion. As a result, the volume of rain (or snow) caught is less, and sometimes much less, than that falling on adjacent open ground. A critical factor is the mean wind speed at the level of the gauge entrance. This problem is known as "raingauge exposure" for which a physical explanation is still incomplete. Rodda (1973) summarised the vast amount of work on raingauge exposure carried out up to that time, commencing with Heberden (1769), and including the famous work masterminded by Symons and Hugh Robert Mill published extensively in British Rainfall (1864-1900). Recently, Sevruk (1982) has described the state of the art, including methods of empirically correcting measured rainfall and snowfall data for exposure effects.

Occasional confusion is caused when the magnitude of raingauge exposure is estimated from wind speeds measured at "standard heights" above the ground. This procedure is acceptable where a logarithmic relationship can be assumed between measured wind speed during rain and the height above ground of the gauge orifice. However some UK gauges are exposed in "turf wall" enclosures in mountainous areas (Meteorological Office, 1969) or surrounded

by vegetation growing to near the level of their entrances, eg gauges surrounded by heather in the Scottish Highlands. Reynolds (1971) points out that these gauges may experience substantially smaller systematic losses compared to a fully exposed gauge. So biases in rainfall totals derived from the standard network of gauges in some mountainous areas of UK may be less severe on average than is sometimes suggested, though many gauges are not adequately protected from the wind.

During the 1970s the International Comparison of National Precipitation Gauges with a Reference Pit Gauge was organised by the WMO Commission for Instruments and Meteorological Observations (CIMO) into the systematic errors of raingauges (Sevruk and Hamon, 1984). This project involved 22 countries, and although much more effective than a previous WMO/CIMO investigation into this topic, the comparisons were hampered by the lack of a theoretical framework for the "exposure" problem. The growing importance to hydrology of systematic errors in rainfall measurements was recognised in 1985 when the first WMO/IAHS Workshop on the Correction of Precipitation Measurements (Sevruk, 1986) was held in Zurich to compare national experiences, discuss the International Comparisons and review new ideas. A preliminary version of the research reported here was presented at the Zurich Workshop (Folland 1986a, b).

The raingauge exposure problem is important in meteorology. Rodda and Smith (1986) have pointed out that the amount of acid deposition by rain may be systematically underestimated due to the systematic losses of rainfall volume from the special but cylindrically shaped gauges used to collect acid rain. In UK these gauges are normally exposed with their orifices at 1.0 m to 2.2 m above the ground so that their wind-induced losses will tend

to exceed those of standardly exposed cylindrical gauges with their orifices at 0.3 m. Also very important is the need to measure rainfall over the oceans more accurately to support climate studies. Satellite estimates of ocean rainfall still have considerable errors and require calibrating against more accurate "ground truth" data (eg Austin and Geotis, 1980). Unfortunately, ground truth data is usually only available for limited places eg some islands. The World Climate Research Programme (WCRP) has placed increased emphasis on the need for ground truth measurements of rainfall over the tropical oceans to support the Tropical Oceans and Global Atmosphere [TOGA] project (WMO, 1986a) and other studies of the global climate (WMO, 1986b). In the latter document the WCRP Workshop on Precipitation Data Requirements make a plea for sufficient acceptably accurate point rainfall measurements over the oceans to calibrate satellite rainfall data (p 28, their underlining):- it would help if actual raingauges were developed that could be used on ships.

The best location for a gauge on a ship is being investigated by the WMO Working Group on Satellite Observing Systems for Climate Research (Gower, Personal communication and WMO, 1986c). The chief concerns are the potentially serious influence of the ships themselves on ambient airflow, and therefore even on the catch of a "perfect" raingauge, and the contaminating effects of sea spray.

There is also an increasing need to correct historical precipitation data for their systematic errors to support studies of long-term changes in precipitation. This is especially necessary in windy or snowy climates. Thus positive corrections for wetting errors were introduced in USSR in 1966 (largest in summer) and for raingauge exposure in 1970 (largest in

winter) (Golubev (1979, Sevruk (1982)). Lack of allowance for these substantial changes of procedure may have affected the homogeneity of long time series of precipitation for the USSR shown by Bradley et al, (1987).

A quantitative theory of raingauge exposure is now developed, supported by extensive field experiments, and a new design of raingauge is proposed that should have substantially lower systematic losses of rainfall volume in the high winds commonly found on moving ships, (Verploegh 1958, WMO 1986b), and over exposed areas on land. The new gauge may also help with the very difficult problem of measuring snowfall.

2. AIRFLOW AROUND A CYLINDRICAL RAINGAUGE

Turbulent airflow normal to an upright cylinder like a raingauge is only partly understood and is complex on short time scales. Another problem concerns the extent to which laboratory experiments on the airflow around raingauges, such as those in a wind tunnel, can be trusted to explain the behaviour of a raingauge placed in the free atmosphere. An important factor discriminating between airflow patterns around small objects like the raingauge cylinder is the Reynolds number, Re:

$$Re = \frac{\rho' L \bar{u}_o}{\mu} \qquad (1)$$

L is a characteristic length of the object; for flow normal to an upright cylinder, L = D, the diameter of the cylinder, and $\bar{u}_o$ is the mean incident velocity of the flow. ρ', the air density and μ, the viscosity of air, vary little over most of the earth's surface. Re is a measure of the ratio of the inertial to viscous forces associated with the flow; its use as a

scaling factor is a consequence of the principles of dynamical similarity in turbulent flow theory. When Re is very low, the airflow tends to be laminar, but at higher Re flow around an object is mainly or wholly turbulent. Only turbulent flow is of practical interest. The mean pattern of turbulent flow around raingauges may slowly change as Re increases but should be similar for a given value of Re. Cylindrical gauges of differing diameter or rim height above ground level should therefore experience a similar mean wind flow pattern across their orifices for a specific value of Re. The pattern of airflow might also depend systematically on the turbulent structure of the incident airflow which could vary greatly with the surroundings of the gauge. However the general similarity in the values of rainfall losses from cylindrical gauges at a given wind speed (when estimated or measured near rim level) for a wide variety of sites in many countries suggests that site-specific turbulence is not crucial, eg Sevruk and Hamon (1984), Sevruk (1982, 1986).

3. FLOW AROUND AN UPRIGHT CYLINDER OF RAINGAUGE DIMENSIONS

3.1 Laminar flow

Although not of practical importance, insight into the exposure problem can be gained by considering steady laminar flow around an upright cylinder of raingauge dimensions. Standard texts do not describe the flow above the top of an upright cylinder, ie above the raingauge orifice, but we can obtain some idea of flow patterns just below the exterior rim of a gauge. Fig 1, from Eckert and Drake (1972) (ED), shows the air pressure distribution around the circumference of a solid circular cylinder of infinite height and diameter 0.25 m for a wide range of Re. The

"theoretical pressure distribution" shown in Fig 1 is that for laminar flow. Applying Bernouilli's equation to steady airflow incident on the cylinder along an axis passing through its centre at the point (0°) where the axis first intersects its circumference:-

$$P_{0°} = \frac{\rho' u_o^2}{2} + P_o \qquad (2a)$$

because u_o at 0° is reduced to zero.

Halfway around the cylinder (points 90° and 270°) the pressure falls to a minimum:-

$$P_{90°} = \frac{-3\rho' u_o^2}{2} + P_o \qquad (2b)$$

and the flow velocity is $2u_o$. At 180° (the leeward circumference opposite to 0°), $u_o = 0$ again and the air pressure is the same as at 0°.

Thus in laminar flow the wind speed is reduced to zero at the windward and leeward edges of the infinite cylinder circumference and is accelerated to twice its ambient value halfway round the cylinder circumference where the air pressure is lowest.

3.2 Turbulent flow

At very low wind speeds (Re < 100) the flow around the cylinder starts to become turbulent (sub-critical turbulent flow) with separation of the flow streamlines from the leeward surface of the cylinder. A further change to super-critical flow may occur at values of Re near 4×10^5. Pressure distributions for these conditions are also shown in Fig 1.

From another diagram in ED it can be deduced that in sub-critical turbulent airflow normal to a cylinder of diameter 8 cm and of approximately raingauge height (0.4 m) the pressure changes are smaller than those in Fig 1. Pressure rises at 0° to about 0.35 $\rho'\bar{u}^2_o$ above its ambient value and falls to a near constant value of about 0.35 $\rho'\bar{u}^2_o$ below ambient pressure at and beyond 60° (300°). Using Bernoulli's equation for time averaged flow, these observations indicates that the horizontal component of the incident airflow should decelerate to near 0.55 $\bar{u}_o$ just to windward of 0° and accelerate again to about 1.3 $\bar{u}_o$ at and beyond 60° (300°). (Conditions to leeward of the cylinder are of little interest.) Wind tunnel tests of airflow over raingauges to be described in section 4 suggest that the horizontal component of flow just above the gauge is quite consistent with this description. Super-critical flow is not likely to be important for gauges of ordinary diameter, e.g 12.7 cm, where an incident velocity of near 40 ms^{-1} at rim height would be required, (but see conclusions, section 13).

4. WIND TUNNEL MEASUREMENTS OF THE AIRFLOW OVER A 5" RAINGAUGE

4.1 Fields of airflow above a standard 5" gauge

Experiments carried out by Robinson (1968) (RB), partly published in Robinson and Rodda (RR) (1969), and by Helliwell and Green (1974) and Green and Helliwell (1972, 1975) (hereafter HG), have provided most of the data on mean airflow patterns around a 5" gauge. Unfortunately, although HG carefully carried out a wider range of experiments than did RB, HG's and RB's measurements disagree on the difference, $\Delta\bar{u}_o$, between the local mean speed and $\bar{u}_o$. RB's estimates of total wind speed vector $K\bar{u}_o$ in the xz plane through the centre of the orifice at $\bar{u}_o$ = 3.5 ms^{-1} and 8.3 ms^{-1} are

shown in the form of isopleths of k in Figs 2a and 2b; RB's corresponding values of $\Delta\bar{u}_o$ are up to about twice those of HG, though HG report similar patterns of mean air flow.

RB's measurements have been preferred because:

(1) It is now thought (Green, personal communication) that a main cause of the difference between HG's and RB's observations lie in the way they were made. HG estimated $\Delta\bar{u}_o$ at a fixed Eulerian grid of points while RB moved his quite similar hot-wire anemometer probe to follow lines of near constant $\Delta\bar{u}_o$. These procedures can give different results if the isopleths of $\Delta\bar{u}_o$ fluctuate appreciably in space and time. The most important region of fluctuation lies close to the highly sheared turbulent boundary layer placed just above the orifice (see Fig 2a). When $\bar{u}_o$ = 3.5 ms^{-1}, RB shows (Fig 2a) that $\Delta\bar{u}_o$ has a maximum value of 0.37 $\bar{u}_o$ just above the boundary layer which falls very rapidly below the boundary layer until, at rim level net average airflow is small. HG's fixed grid of [Eulerian] measurements is likely to miss the flow maximum because fluctuations of the position of the strongly sheared turbulent boundary layer were on a space scale larger than that of HG's grid length. Neglect of the time varying turbulent structure of the flow will be fully justified when the modelled rainfall losses are compared with observed losses (Section 6).

(2) RB's horizontal flow component maxima of $\Delta\bar{u}_o$ = 0.37 $\bar{u}_o$ for $\bar{u}_o$ = 3.5 ms^{-1} (Re = 3.1 x 10^4) and 0.26 $\Delta\bar{u}_o$ at 8.3 ms^{-1} (Re = 7.4 x 10^4) agree quite well with the estimate of 0.3 $\bar{u}_o$ made in section 3.2. His minimum total horizontal component of $\Delta\bar{u}_o$ occurs about 2-3 cm to windward of the gauge and is about 0.55 $\bar{u}_o$ (total flow velocity 0.94 $\bar{u}_o$ at a positive

angle of $\theta = 55°$ to the horizontal), agreeing with the estimate made in section 3.2.

(3) Serra (1958) also measured, with less reliable instruments, a maximum horizontal flow component of about 1.3 $\bar{u}_o$ above a cylindrical raingauge at a value of Re near 10^5.

RB made no measurements outside the xz plane but Serra (1958) (not shown) and HG ($\bar{u}_o = 6$ ms^{-1}, not shown) demonstrate that variations of $\Delta\bar{u}_o$ in the y direction are slow. They can be neglected in a simplified theory because the area of the gauge orifice experiencing appreciably reduced values of $\Delta\bar{u}_o$ is located near points 90° and 270° and so has a relatively small size. The turbulent, "separated", zone of airflow just above the gauge orifice is shown by RB (Figs 2a and 2b) and HG (not shown) to thicken slowly towards the leeward side of the orifice. HG also suggest that the separated zone slowly thins in the positive and negative y directions.

RB does not indicate how far above the gauge appreciable values of $\Delta\bar{u}_o$ may be found; however HG ($\bar{u}_o = 6$ ms^{-1}) show that the incident flow ceases to be accelerated about 30 cm above the orifice and starts to be perturbed about 50 cm to windward of the gauge. HG also show that the turbulent boundary layer changes its shape when $\bar{u}_o > 5$ ms^{-1}, so that the tendency found at lower speeds for the boundary layer to be closer to the gauge at its leeward rim (180°) than over its centre ceases. Fig 2b (for $\bar{u}_o = 8.3$ ms^{-1}) is representative of HG's results for $\bar{u}_o > 5$ ms^{-1}. Otherwise HG's [Eulerian] measurements show only small changes in the pattern of k from $\bar{u}_o = 1.5$ ms^{-1} to $\bar{u}_o = 15$ ms^{-1}, though slightly larger values of k are observed near $\bar{u}_o = 3$ ms^{-1} than at other speeds.

The airflow is most strongly accelerated close to the windward rim of the orifice as shown in wind tunnel tests by Warnick (1953). Using snow and sawdust as a tracer, Warnick shows that a jet of air adjacent to the (windward) 0° point on the orifice rim is directed upwards and almost parallel to the sides of the gauge [the gauge he tested had sides that sloped gently upwards and inwards toward the orifice]. Continuity of flow requires that air originating from above or below this level be entrained into the jet. This observation is important, since in strong winds most of the smaller raindrops will encounter this region of maximally perturbed flow.

4.1.2 Sensitivity of the wind flow to details of the orifice

RB used photographs of smoke plumes to make the air flow visible near plastic models of 5" gauges. He found that the flow patterns were fairly insensitive to whether the gauge possessed an open or closed orifice or whether the rim was sharp or more rounded. In all cases the vertical components of flow velocity adjacent to the windward rim of the orifice were of comparable size to their horizontal cocmponents. So the precise shape of the orifice rim is likely to have only a secondary (though not completely negligible) influence on the pattern of air flow over a cylindrical gauge and can be neglected in a simplified theory.

5. NUMERICAL MODELS OF 5" RAINGAUGE LOSSES

The main part of the first model (Model 1) is two dimensional. The gauge is assumed to have a diameter of 12.7 cm with its rim 30 cm above the

ground. An observed wind field is defined in the xz plane and all model calculations are carried out within it. Three dimensional losses are estimated from the explicit two dimensional calculations using geometrical considerations. It is then shown (section 6) that an even simpler quasi-analytical model (Model 2) gives quite similar losses, indicating the general robustness of the results.

5.1 Model Wind field (both models)

Figures 3a shows the mean flow speed factor k used in the model and Figs 3b the angles of flow to the horizontal, θ, for $0 < \bar{u}_o \leq 5$ ms^{-1} and $10 \leq \bar{u}_o \leq 20$ ms^{-1} respectively. Up to 15 cm above the gauge, the values of k were based on RB's measurements at $\bar{u}_o = 3.5$ ms^{-1} (Fig 2a), with allowance for a mean logarithmic wind shear in the wind flow above the gauge and use of Warnick's observations close to the windward rim of the gauge. The reference level for the incident wind speed, $\bar{u}_o$, was chosen to be 5 cm above the orifice rim. This is about the level of the mean maximum airflow velocity close to the orifice. The logarithmic wind speed profile was defined by:-

$$\bar{u} = \bar{u}_o \frac{\ln H}{\ln 35} \qquad (3)$$

where H = height in cm above the ground. Equation (3) assumes a surface roughness length of 1 cm and a zero displacement height but the wind profile is insensitive to other reasonable choices of roughness length (0.25 -3 cm) and displacement height. HG's measurements were used to extend the k field to 35 cm above the gauge, at which height the ambient logarithmic profile gives $\bar{u} = 1.17\ \bar{u}_o$ and the gauge ceases to disturb the flow.

Figs 3a, and especially 3b, differ somewhat from corresponding fields of k and θ given in Folland 1986a. Besides providing an additional field of angles of the wind flow for $\bar{u}_o \geq 10$ ms^{-1}, care has been taken to ensure that the implied mean wind vectors do not have significant components in the y direction. Below $\bar{u}_o = 10$ ms^{-1}, this has been achieved by applying the equation of continuity to the initial estimates of θ shown in Folland (1986a), while keeping most values of k unchanged:-

$$\frac{\partial[k\bar{u}_o \cos\theta]}{\partial x} + \frac{\partial[k\bar{u}_o \sin\theta]}{\partial z} \cong 0 \qquad (4)$$

Beyond the limits of Figs 3a and 3b, θ=0 and k was calculated using equation 3. Overall, the smoothed values of θ and $\bar{u}$ imply a small net divergence in both positive and negative y directions above the windward half of the gauge (about 2% of the mass flux) and a small net convergence above the leeward edge. This seems physically reasonable.

5.2 Raindrop size distributions

The model was integrated for a wide range of raindrop sizes and for six frequency distributions of raindrop size derived from two families of drop diameter frequency distributions. These have been selected to be those of Best (1950) and Ulbrich (1983). The motion of a given raindrop is assumed not to affect that of other raindrops, so the drop paths have been modelled individually.

5.2.1 Best's dropsize distributions

Best found that observations of the frequency of raindrop sizes in several countries could be adequately represented by

$$1-F(d) = \exp\left[- \left(\frac{d}{a}\right)^{n} \right] \quad (0<F(d)<1) \qquad (5)$$

F(d) is the fraction of the total rainfall volume comprised of drops of diameter $\leq$ d; a and n are constants where a = f(R) and R is the rate of rainfall in mm h^{-1}. In UK, n appeared to vary on average from about 2 (lowland regions) to 2.5 (upland regions). The better-known Marshall-Palmer drop-size distribution, (Marshall and Palmer (1948)), is generally thought to calculate a frequency of the very small drops that contribute most to exposure losses which is too high. This distribution corresponds closely to n=1.85 (Best, 1950). From Best (1950) and Mason (1971), a is assumed to be given by:-

$$a = \frac{R^{0.23}}{(0.69)^{n}}^{-1} \qquad (6a)$$

Substituting (6a) into (5) gives:-

$$d = \left[- 1.45 \, R^{0.23n} \, \ln(1-F(d)) \right]^{n^{-1}} \qquad (6b)$$

The majority of integrations were made for n=2. This enabled comparisons to be made with a statistical model of rainfall losses in the low rainfall, lowland conditions of Denmark given by Allerup and Madsen (AM) (1980). Fig 4a illustrates relationships between F(d) and d for R = 0.1, 1 and

10 mm h^{-1} for n=1.85 and n=2.25. The larger the value of n, the narrower the drop size distribution.

5.2.2 Ulbrich's gamma drop size distributions

This generalised form of the gamma drop size distribution (Ulbrich, 1983) is given by:-

$$F(d) = \frac{\lambda^{(4+\mu)}}{\Gamma(4+\mu)} \int_0^d d^{(3+\mu)} \exp(-\lambda d)\,dd \qquad (7)$$

where $\lambda = [33.31\ N_o\ \Gamma(4.67+\mu)]^{(4.67+\mu)^{-1}}\ R^{-(4.67+\mu)^{-1}}\ cm^{-1}$,

$N_o = 6 \times 10^4 \exp(3.2\mu)\ m^{-3}\ cm^{-1-\mu}$ and d is in cm.

The above value of N_o is based on an analysis by Ulbrich of 69 radar reflectivity - R relationships given in Battan (1973). μ is a shape parameter: μ=-1 corresponds to a broad drop size distribution with more small and large drops than given by an exponential drop size distribution while μ=1 corresponds to a correspondingly narrower distribution (Fig 4b). Ulbrich suggests that μ=0 to μ=1 is typical of widespread stratiform rainfall while μ=-1 is more typical of orographically enhanced rainfall. Showers may have a very broad range of positive and negative values of μ. Integrations were carried out for μ=-1, 0 and 1, a wider range of drop size distributions than those used in section 5.2.1.

5.3. Equations of motion for falling raindrops

Consider a raindrop of diameter d falling through air whose vertical velocity relative to that of the air is $v_r(d)$ and whose horizontal velocity

relative to that of the air is $u_r(d)$. Neglecting the very small buoyancy forces, the net downwards force F_z is:

$$F_z = mg \pm f(^1/_2\rho' v_r(d)^2) \qquad (8a)$$

m is the drop mass, g is the acceleration due to gravity and $\pm f(^1/_2 \rho' v_r(d)^2)$ is a function which depends on the vertical component of relative air velocity. In equation 8a, the second term is subtracted (added) if the drop is falling (rising) relative to the air.

The only horizontal force is that due to the horizontal component of the relative speed of the air (taken as positive if directed in the positive x direction):-

$$F_x = \pm f(^1/_2 \rho' u_r(d)^2) \qquad (8b)$$

Using suitable timesteps, the model calculates the changing net vertical and horizontal components of these forces on a given drop and thus its changing vertical and horizontal components of velocity. Introducing the drag coefficient of the drop, C_D, and expressing the drop mass in terms of drop density and volume, the net force on the drop in the downward z direction, F_z, becomes, in consistent units:-

$$F_z = \frac{1}{6}\Pi\rho_w d^3 \frac{dv_z(d)}{dt} = \frac{1}{6}\Pi \rho_w d^3 g - C_D \frac{\Pi d^2}{8} \rho'(v_z(d)+w)|v_z(d)+w| \qquad (9)$$

ρ_w is the density of water, $v_z(d)$ is the vertical component of velocity of the drop, positive when directed <u>downwards</u>, and w is the vertical velocity of the air, positive when directed <u>upwards</u>.

Similarly the net force along the x axis in the positive x direction is:-

$$F_X = \frac{1}{6}\pi\rho_w d^3 \frac{dv_x(d)}{dt} = \frac{C_D \pi d^2}{8} \rho'(u-v_x(d))|u-v_x(d)| \qquad (10)$$

$v_x(d)$, the horizontal component of drop velocity, is positive when directed in the positive x direction (downwind) and u, the horizontal component of air velocity, is positive when similarly directed.

The model time steps Δt were arranged to correspond to the passage of drops between horizontal planes placed at a variable distance Δz apart given by:-

$$\Delta t = \left|\frac{\Delta z}{v_z(d)}\right| \qquad (11)$$

$v_z(d)$ is the vertical velocity of the drop immediately prior to an increment of time Δt. From equations (9) — (11) the changes $\Delta v_z(d)$ in $v_z(d)$ and $\Delta v_x(d)$ in $v_x(d)$ during a time increment Δt are:-

$$\Delta v_z(d) = \left|\frac{g}{v_z(d)}\right| |\Delta z| - \frac{3}{4}\frac{C_D}{d}\frac{\rho'}{\rho_w} |\Delta z| \frac{(v_z(d)+w)}{|v_z(d)|} |v_z(d)+w| \qquad (12)$$

$$\Delta v_x(d) = \frac{3}{4}\frac{C_D}{d}\frac{\rho'}{\rho_w} |\Delta z| \frac{(u-v_x(d))}{|v_z(d)|} |u-v_x(d)| \qquad (13)$$

Refinements were made to equations (12) and (13) to maintain computational stability. In equation (12), $v_z(d)$ was replaced by $v_z(d)_1 + 2 \times 10^{-3}$, where $v_z(d)_1$ is the velocity of the drop before addition of the increment $\Delta v_z(d)$ (measured in ms^{-1}). In equation (13), $v_z(d)$ was replaced by $^1/_2$ $[v_z(d) + v_z(d)_1 + 2 \times 10^{-3}]$.

The change in the position of the drop on the x axis after a time Δt is then:-

$$\Delta x = \frac{(v_x(d)+v_x(d)_1)|\Delta z|}{|v_z(d)+v_z(d)_1|} \qquad (14)$$

Δz was set to 5×10^{-3} m in the undisturbed flow and decreased to maintain computational stability when the terminal velocity of the drop decreased.

5.3.2 The raindrop drag coefficient, C_D

The value of Re appropriate to the current velocity of the drop was calculated from equation (1) by replacing $L\bar{u}_o$ by $d|w-v_z(d)|$ for the vertical component of drop velocity and by $d|u-v_x(d)|$ for the horizontal component.

Values of C_D (for an air temperature of 7.5°C and air pressure of 1000 mb) were made as consistent as possible with terminal velocities of raindrops tabulated by Mason (1971). Subject to a minimum value of $C_D = 0.55$, the slightly revised formulations for C_D compared to those given in Mason (1971) became:-

$$Re<0.01 \qquad C_D = 2547 \qquad (15a)$$

$$0.01 \leq Re \leq 2 \qquad C_D = 1.06 \left[\frac{24}{Re} + 2.4\ Re^{-0.045}\right] \qquad (15b)$$

$$2 \leq Re \leq 21 \qquad C_D = 1.06 \left[\frac{24}{Re} + 2.64\ Re^{-0.19}\right] \qquad (15c)$$

$$21<Re \qquad C_D = 1.06 \left[\frac{24}{Re} + 4.536\ Re^{-0.368}\right] \qquad (15d)$$

Equations 15 a-d give terminal velocities of raindrops in still air at the air temperature and pressure described above that agree to within 2% with those of Mason over the range $0.1<V_t<8.3\ ms^{-1}$.

5.4 Computed rainfall losses

5.4.1 Two dimensional losses for Model I

All raindrops were started at their terminal velocities from a reference level 35 cm above the orifice plane, placed at a variable distance to its windward. Since the terminal velocity of the drop can fall to near zero (or become negative), tests were devised to ensure that the first drop of a given mass fell to windward of 0° at the level of the gauge orifice.

Drops of a given mass released from the reference plane were uniformly spaced apart in the x direction at a distance of 0.635 cm. [This distance is $^1/_{20}$th of the orifice diameter.] The paths of each drop were followed until tests showed that all drops released from the reference plane from positions progressively nearer the gauge fell to leeward of the 180° point at rim level.

5.4.2 Three dimensional losses for Model I

The variation of orifice width in the y direction was allowed for as follows. Consider the true incident rainfall that is contributed by all drops of fixed diameter d. The fraction of this amount which is represented by one drop of that size falling onto the x axis is given by:-

$$f_d = \frac{[40.3225\ 10^{-4} - x^2]^{1/2}}{0.99746} \qquad (16)$$

where x = 0 at the orifice centre, x = -6.35 cm on the windward rim (0°) and x = 6.35 cm on the leeward rim (180°). f_d is a maximum at the centre of the gauge and zero at 0° and 180° and sums to unity for 20 drops evenly spaced in x.

The total collected rainfall that is made up of drops of diameter d and expressed as a fraction of the true incident rainfall is:-

$$C_d = \sum_{i=1}^{m_d} f_d \qquad (17$$

where m_d is the number of drops falling onto the x axis within the orifice. The error due to the finite spacing of the drops is negligible for an initial drop spacing of 0.635 cm. C_d can exceed unity even if m_d = 20 if the drops are concentrated along the x axis towards the central, widest part of the orifice.

The total rainfall collected, C, was calculated by summing values of C_d for 41 sets of drops, each of fixed diameter covering the complete drop size distribution. Each set of drops is associated with a fixed fraction g_d of the total incident rainfall; g_d can be calculated from F(d) with the aid of equations 6b or 7a. C is given by:-

$$C = \sum_{d=1}^{41} g_d C_d = \sum_{d=1}^{41} g_d \sum_{i=1}^{m_d} f_d \qquad (18)$$

g_d was chosen to be 0.005 for $0.0025 \leq F(d) \leq 0.0975$; 0.01 for $0.105 \leq F(d) \leq 0.195$; 0.05 for $0.225 \leq F(d) \leq 0.475$ and 0.1 for $0.55 \leq F(d) \leq 0.95$. For Best's drop size distribution with n=2, this set of values of g_d

corresponds to a range of drop diameters from 0.06 mm to 2.08 mm and illustrates the wide range of drop diameters that must be considered in the raingauge exposure problem.

5.4.3 Losses for Model II

Model II is reduced to a quasi one dimensional calculation but uses the same equations of drop motion. We first note the position x_1 on the x axis at orifice level nearest to 0° (Fig 5) through which the first drop of a given diameter falls. A second drop is released from the reference plane 12.7 cm nearer the gauge (12.7 cm is the orifice diameter) and its position x_2 is noted as it falls through the orifice plane. C_d is calculated from x_1 and x_2 alone with the aid of Figure 5. The rainfall that would have been incident into the orifice in the absence of distortion of the flow is assumed to fall (a) into the gauge and (b) into a downstream region shaped like half an ellipse which includes the leeward half of the gauge. The major semi-axis of the elipse has length a defined by x_1, (see Fig 5), and the minor semi-axis has length b equal to the radius of the gauge. An ellipse is a reasonable shape for the collecting area: drops falling through 90° and 270° make no contribution to the rainfall caught, while those falling through the x axis will be displaced most since the region of disturbed flow is widest here and extends furthest in the positive x direction. Raindrops are imagined to be uniformly distributed between x_1 and x_2 and in the $\pm y$ directions. This is the most severe simplification in Model II.

C_d is then given by the ratio of the area of the gauge orifice to that of the total shaded area in Fig 5:-

$$C_d = \frac{2a}{a+b} \qquad (19)$$

Note that $C_d > 1$ if $a < b$. If no drops of a given diameter entered the orifice between -8.35 cm $< x_1 < 0$ cm ($x=0$ is at the centre of the gauge) then C_d was set to zero. Because it was difficult to arrange for drops to fall exactly through 0°, the nearest drop was considered to be at 0° if it lay in the range -7.6 cm $< x_1 < 0$ cm; the vast majority actually lay in the range -7.6 cm $< x_1 < -6$ cm. Altering these limits by 1 or 2 cm had little effect on C_d despite the fact that in principle the shaded areas in Fig 5 become slightly displaced from their nominal relationship to the position of the orifice. C was calculated as in section 5.4.2.

6. RESULTS AND COMPARISONS WITH OBSERVATIONS

Fig 6 shows the calculated percentage of incident rainfall 100 C(%) collected by a 5" gauge orifice from Model I for a range of drop diameters from d = 0.04 mm to d = 3.5 mm and for $\bar{u}_o$ = 0.5, 2, 5 and 20 ms^{-1} (solid lines). C generally increases, as expected, as d increases. At a given value of $\bar{u}_o$ the change from C = 0 to C ~ 1 over a fairly narrow range of d is notable; this range widens as $\bar{u}_o$ increases. C is sometimes fractionally larger than unity e.g. at $\bar{u}$ = 0.5 ms^{-1} at some low values of d (not shown). For d > 2 mm, simulated losses are less than 1% of drops even at $\bar{u}_o$ = 20 ms^{-1}, though for d < 0.4 mm all drops are lost at this speed. Although C usually decreases as $\bar{u}_o$ increases for a given value of d, this is not always quite true for low wind speeds and small drop diameters. These results appear to disagree strongly with losses calculated for a slightly different gauge by Mueller and Kidder (1972) for d ≧ 1 mm and high

values of $\bar{u}_o$. Their calculated losses in these conditions were much larger than those shown here but further comparison is difficult as Mueller and Kidder did not publish details of their wind field.

Fig 7a shows the modelled percentage losses of true incident rainfall, 100 [1-C] for Model 1 as a function of $\bar{u}_o$ for $0.1 \leq R \leq 10$ mm h^{-1} and for Best's drop size distribution with n = 2 and (selectively) n = 2.25. Modelled losses are compared with AM's 1980 statistical model of the observed losses of rainfall from cylindrical Hellman gauges in Denmark, (dashed lines) for values of $\bar{u}_o$ up to 15 ms^{-1}. AM's statistically modelled losses were derived from daily values of R and $\bar{u}_o$. They tabulate corrections to the observed catch for wind speed measurements at 10 m above ground at exposed sites which have here been converted to losses of the true catch for values of $\bar{u}_o$ estimated at 5 cm above the Hellman gauge rim (1.55 m above ground) using Equation 3.

Fig 7b shows a similar set of results using Ulbrich's gamma drop size distribution for μ = -1, 0, 1 and for R = 0.1, 1 and 10 mm h^{-1} only. A value of μ near 0 (section 5.4.3) may provide the most appropriate overall comparison with AM's model. Ulbrich's distributions tend to give a small increase in collected rainfall above the incident value for $\bar{u}_o < 1$ ms^{-1}.

Given the uncertainties in the numerical model wind field, in the formulation of appropriate drop size distribution and the fact that AM's results refer to a different (cylindrical) gauge (diameter 16 cm, orifice height 1.5 m), the general agreement between Model I and AM's model for both families of drop size distribution over this wide range of $\bar{u}_o$ and R is very encouraging. [Systematic small differences between the true wind

field over the Hellman gauge collector and that over the standard 5" collector may exist because the vertical windshear may be slightly less over the more elevated Hellman gauge orifice.] AM's model and the numerical model are likely to be most secure for $\bar{u}_o \leq 5$ ms^{-1} and here the agreement is especially good. Best's drop size distribution formulae are likely to be most appropriate near 1 mm h^{-1}, average conditions in UK.

Fig 7c shows that losses predicted by the very simple quasi-analytical (Model II) are only in slightly worse agreement with AM's results than is Model I. This indicates the robustness of the models and the fact that the exposure losses are essentially due to:

(a) The (nominally) complete loss of a range of the smallest raindrops at a given value of $\bar{u}_o$ (Model I and Model II give similar results).

(b) The divergence of the remaining drops that results from the horizontal acceleration of the flow over the gauge and the existence of strong vertical components of air velocity that decrease drop momentum and increase their residence time in the divergent flow. Details of exactly where the diverging drops fall into the gauge are seen from the small differences between Figs 7a and 7c to be of mainly minor importance as only Model I attempts to make a realistic calculation of this factor.

Figs 7a and 7b show that, expressed as a fraction of the incident rainfall, the predicted losses increase almost linearly with $\bar{u}_o$ up to about $\bar{u}_o = 5$ ms^{-1}, though at very low values of R the relationship between $\bar{u}_o$ and R is

non-linear at all values of $\bar{u}_o$. (Low values of R contribute relatively little to total rainfall). Linearity is also absent for $\bar{u}_o < \sim 0.8$ ms^{-1} where the catch is insensitive to $\bar{u}_o$ otherwise linearity is best for corrections to the observed rainfall and tends to extend to higher values of $\bar{u}_o$. At higher values of $\bar{u}_o$ modelled losses increase at a slower rate, though above 10 ms^{-1} the losses again increase nearly linearly. When $\bar{u}_o >$ 5 ms^{-1}, AM's model (based on relatively few data at high values of $\bar{u}_o$) gives larger losses than the physical model except at very high and very low rainfall rates and exhibits a more closely linear set of loss curves.

Further support for the predictions of all the above models in UK conditions is shown in Fig 8. Fig 8 shows observed losses 100 [1-C] calculated by Rodda and Smith (RS) (1986) for 5" standard gauges with rims exposed at 30 cm and based on about 120 station years of data from 17 stations; ground level gauges provided the reference data. Although the average rate of rainfall, $\bar{R}$, varied a little from station to station, each point is based on several years of observations. The true value of $\bar{R}$ probably varied between about 1.0 mm h^{-1} at the driest stations and about 1.5 mm h^{-1} at the wettest. Losses at the most elevated stations may be influenced (increased) by the collection of appreciable amounts of sleet or snow, though very snowy winters were avoided. The mean wind speeds shown in Fig 8 were measured at 2 m above the ground in all weather conditions. Numerical model wind speeds were converted to speeds at 2 m assuming a logarithmic wind profile, z_o=1 cm and zero displacement height. Sevruk (1982) suggests that in climatic conditions like those of UK the mean wind speed in rain (over a lengthy period) is about 1.13 times that averaged over all weather conditions. This effect is compensated almost completely by AM's (1979)

suggestion that estimates of rainfall loss over short periods for given values of $\bar{u}_o$ and R (such as are effectively made by the numerical model) may over-estimate long-term losses for long-term average values of $\bar{u}_o$ and R by 10-15%. Appendix I confirms that losses modelled at specific values of R and $\bar{u}_o$ should be quite similar to those for similar values of $\bar{R}$ and $\bar{u}_o$ averaged over a large number of observations and should be nearly independent of the frequency distributions of R and $\bar{u}_o$. So we can directly compare the physical model predictions to RS's reported losses. For n=2, and R = 1 mm h^{-1}, Model 1 agrees quite well with RS's loss curve. Model 1 simulations using Ulbrich's gamma drop size distribution are also shown and hint that at RS's windiest (wettest and most exposed) stations a value of $\mu \sim -1$ agrees best with the measured losses. Thus the orographic component of rainfall present at these mountain stations (which should increase the proportion of small drops) could be important in increasing losses of rainfall to values appreciably higher than those expected from lowland stations.

Table I is taken from unpublished data in HG (1974). HG calculated the mean rate of rainfall and mean wind speed at gauge rim height (measured in rainfall only) for 42 rainfall events (including thunderstorms) over an experimental plot in the Chiltern Hills near Medmenham, Buckinghamshire, UK. Standard 5" gauges were exposed with their rims at several heights between 30 cm and 3 m above the ground. HG noted that the constituent 10-minute wind speeds followed a highly skewed log-normal frequency distribution (which should have little effect on the results Appendix I). The overall mean rate of rainfall was about 1 mm h^{-1}. The reported wind speeds, measured at gauge rim height, have been adjusted to a height 5 cm above the rim assuming a roughness length of 1 cm and zero displacement

height. Assuming R = 1 mm h^{-1}, Table I shows good agreement between modelled and observed losses for n = 2 and $\mu \sim -0.5$.

TABLE I

ANALYSIS OF 42 RAINFALL EVENTS AT MEDMENHAM USING HELLIWELL AND GREEN'S UNPUBLISHED DATA

HEIGHT OF GAUGE rim (m)	0.3	1.0	2.0	3.0
Mean wind speed 5 cm above gauge ms^{-1}	1.40	1.88	2.17	2.26
Observed loss %	4.6	5.4	6.8	7.3
Calculated loss %				
R = 1 mm h^{-1}, n=2	4.0	5.7	6.9	7.2
R = 1 mm h^{-1}, μ=-1	4.4	7.3	9.1	9.6
μ=0	1.7	3.6	4.7	5.1

7. Implications of the model results for field experiments and raingauge design

Past observations of rainfall losses (1-C) versus $\bar{u}_o$ (using ground level gauges as a reference) have sometimes shown considerable scatter,

especially when individual daily or shorter period rainfall measurements have been analysed. This is probably due to the strong sensitivity of 1-C to R. R has often been neglected as an observed parameter in field experiments. Figs 7a-7c indicate that at $\bar{u}_o$ = 2 ms^{-1} the expected loss at R=0.5 mm h^{-1} is about twice that at 2 mm h^{-1} so that for many sites daily and shorter time scale rainfall losses are likely to be more affected by variations in R than by variations in $\bar{u}_o$. Variations in the underlying drop size distribution will further weaken the correlation between daily values of 1-C and $\bar{u}_o$.

A partial allowance has sometimes been made for the variation of 1-C with R. Sevruk and Hamon (1984) analysed the results of the WMO International Comparison of National Precipitation Gauges with a Reference Pit Gauge by stratifying half-daily rainfall totals according to whether the estimated value of R was above or below 0.03 mm min^{-1} (1.8 mm h^{-1}). A parameter N was calculated which describes the fraction of such rainfalls with a mean R < 1.8 mm h^{-1}. This procedure was recommended in the USSR by Bogdonova (1966). Figs 7a-7c indicate that Bogdonova's procedure may only be mildly helpful as the sensitivity of half-daily losses to R will often be too great to be described by just one threshold value of R. However Sevruk and Hammon did find a weak relationship with N in the sense expected from Figs 7a-7c. RS's results (reported in section 6) were based on an average of several years data at each station so largely overcame the problem of varying values of R. This is why their linear correlation coefficient between $\bar{u}_o$ and 1-C has the high value of 0.84.

The foregoing results indicate that a cylindrical raingauge is a poor instrument for estimating rainfall "ground truth" in any very exposed

place. When a typical ship's speed is included (7-12 m s^{-1}) rainfall measurements in the generally moderate winds of the tropics may be unreliable. RR were aware that a conically-shaped collector might be an improvement, much as suggested by Verploegh (1958), who carried out field trials with a conical gauge on a ship. In section 8 we consider why a conically-shaped collector might exhibit reduced losses and calculate the potential losses of this collector. A new collector is then designed and field tests of the new collector described.

8. COLLECTORS SHAPED LIKE AN INVERTED CONE

8.1 Why an inverted cone might distort the wind field less than a cylinder

Using the notation of section 3.1, we can write Bernoulli's equation for steady laminar airflow approaching an inverted cone of semi-angle ϕ (to the vertical) along an x axis passing through the centre of the base of the inverted cone. Let the air strike the cone just below the 0° point on the windward rim. The incident air speed along the x axis is reduced from u_o to a component $u_o \sin\phi$ so that:-

$$P_0° = P_o + \rho' \frac{u_o^2}{2} [1-\sin^2\theta] \qquad (20a)$$

Thus in laminar flow the pressure increase just below the windward rim of the inverted cone is less than that for the cylinder. If $\phi = 45°$ then:-

$$P_0° = P_o + \frac{1}{4} \rho' u_o^2 \qquad (20b)$$

ie $P_0°$ is increased above the ambient value by $^1/_4\ \rho' u^2_o$, ie only half that for the cylinder. If, as for a cylinder of raingauge dimensions, the drop in pressure is assumed to be twice the increase above ambient at 0° and this drop occurs between 0° and 60° (section 3.1) then the pressure rise above ambient at 0° for a 45° inverted cone would be about $0.18\ \rho' \bar{u}^2_o$. The downstream pressure at 60° is then $0.18\ \rho' u_o^2$ below ambient. If this pressure drop also occurs <u>just</u> <u>above</u> the orifice rim, the mean horizontal component of the wind flow would be to about $0.80\ \bar{u}_o$ near 0° and $1.17\ \bar{u}_o$ near and beyond 60°.

For convenience, we shall describe inverted conical collectors in terms of their value of α where $\alpha = 1-\phi$. α is therefore the angle between the horizontal plane and the sloping side of the inverted cone. Consider a quantity Q defined by:-

$$Q = \frac{(P_o° - P_o)\alpha}{(P_o° - P_o)_{90°}} \qquad (21)$$

Although Q provides only a qualitative index it suggests that an inverted cone with $\alpha = 30°$ ($Q = 0.25$) might disturb the wind flow considerably less than does a cylinder ($Q=1$) and appreciably less than does an $\alpha = 45°$ cone ($Q=0.5$). So we have carried out numerical simulations of 1-C for an $\alpha = 45°$ conical gauge using the wind tunnel measurements made by RB and and partly published in RR (1969). Field experiments were also carried out using a quasi-conical collector with an effective $\alpha = 35°$ (nominal value of $Q = 0.33$)

8.2 Wind field over the inverted 45° cone of diameter 5"

As with the 5" gauge measurements, the field of total mean air flow velocity vector above the orifice, $k\bar{u}_o$, is better defined than that of its mean angles to the horizontal, θ. Initial estimates of the θ field over a conical gauge shown in Folland (1986b) have been smoothed using the equation of continuity (equation 4, section 5.1). Smoke plume photographs for $\bar{u}_o \leq 5$ m/sec were used to provide additional estimates of θ. The values chosen were biased to be slightly greater than those indicated by the photographs so as to provide minimum estimates of the improvement in catch that might result from using a conical collector.

The model wind field (Figs 9a and 9b), was estimated to a height of 30 cm above the orifice where it was considered to be unperturbed. RB showed that the maximum value of k decreased considerably between $\bar{u}_o = 3.5$ m s^{-1} (1.29) and $\bar{u}_o = 8.3$ m s^{-1} (1.16) so a compromise maximum value of k = 1.25 was chosen. The minimum horizontal component of flow to windward of 0° is 0.90 $\bar{u}_o$ ($k = 0.98$, $\phi = 24°$).

8.3 The Model Physics

Except for the wind field, the model was constructed in the same way as Model 1 of the 5" gauge. See section 5 for details.

9. RESULTS

Fig 10 shows 100 C as a function of wind speed and drop size for $\bar{u}_o$ = 3 and $\bar{u}_o$ = 10 ms^{-1} and the corresponding 5" gauge losses. For these and all other values of $\bar{u}_o$ except $\bar{u}_o$ = 0.5 ms^{-1} (not shown), the losses from the 45° conical gauges tend to be much less than those for the 5" gauge for the smaller drop sizes. The range of drop diameters having losses of 100% is larger than for the 5" gauge (except at $\bar{u}_o$ near 0.5 ms^{-1}). Fig 11 shows 100 [1-C] as a function of $\bar{u}_o$ (maximum value 15 m s^{-1}) and R for Best's drop distribution parameter n=2 and, selectively, for n=2.25. There is a clear reduction in the modelled losses compared with those of the 5" gauge (Fig 9) except at $\bar{u}_o$ < 0.75 ms^{-1}. Losses for n=2.25 are similar to those for n=2. The calculated ratio, r, of 45° cone gauge losses to 5" gauge losses (taken from Model I) steadily reduces below unity as $\bar{u}_o$ increases, falling to 0.34 for R=1 mm h^{-1} at 15 ms^{-1}. This is shown in Table II.

TABLE II RATIO, r, OF COMPUTED 45° CONICAL AND 5" GAUGE RAINFALL LOSSES DUE TO WIND using n=2

	R		
$\bar{u}_o$	0.1 mm h^{-1}	1.0 mm h^{-1}	10 mm h^{-1}
0.5	1.14	1.18	0.46
1	0.62	0.62	0.58
2	0.49	0.51	0.52
5	0.44	0.41	0.41
15	0.42	0.34	0.32

In reality collection efficiencies may be less than shown above for a small diameter conical gauge because rain will tend to splash out of a purely conical collector, especially heavy rainfall, (though as explained in section 8.2, these calculations may in other respects be pessimistic). Fig 11 also shows that the modelled conical gauge loss curves are strongly non-linear functions of wind speed for values of $\bar{u}_o < 7$ ms^{-1}. Appendix I shows that this non-linearity prevents a straightforward estimate of long-term mean losses from a 45° conical gauge from Fig 11. This problem may not be important if the losses are really much less than those for a 5" gauge since the small corrections would only have to be approximately estimated.

10. A SUGGESTED NEW RAINGAUGE COLLECTOR

Fig 12a shows a design for a "first-guess" new collector having the minimum recommended diameter of 25 cm. This includes near-vertical sides to minimise splash-out, and an equivalent $\alpha = 35°$. The new collector is named the "flat champagne glass". As the collector diameter is increased, splash-out losses could reduce almost linearly for a fixed height of the side walls. However for a fixed collector shape the losses should reduce substantially faster since the height of the near vertical sides also increases in proportion to diameter.

Fig 12b shows a modified collector with $\alpha \cong 40°$ and larger diameter which should be more satisfactory in the high winds on moving ships. The near vertical sides are 11 cm high in accordance with the design of the 5" gauge. It would be desirable to decrease α further by making the diameter

of the gauge even larger. A reason for considering this is that for cylinders of raingauge height, supercritical flow sets in for $Re > 4 \times 10^5$. Thus we may imagine that the average pressure drop across the champagne glass might substantially decrease for a large enough diameter in supercritical flow though there could be an increased pressure drop within its windward half as in Fig 1. The net effect may be to give reduced losses in supercritical flow. If a transition value of $Re = 4 \times 10^5$ is applied, a champagne glass gauge with a diameter of 1 m would show a transition to supercritical flow at $\bar{u}_o$ near 6 ms^{-1}, below the speed of most ships. Wind tunnel tests would be needed to confirm these speculations.

Reduced "wetting" errors may also be a minor advantage of a flat champagne glass gauge (Sevruk, 1982, gives a detailed discussion of wetting errors). Compared to 5" or Hellman collectors, wetting losses for a "flat champagne glass" collector should be less because the ratio of internal collector surface area to orifice area is less. The reduction depends on the precise shape of the "champagne glass", but a typical value could be 30%-50%. The net reduction in wetting errors will be less because of the unchanged influence of the wetting errors of the discharge pipe and measuring cylinder.

11. FIELD TRIALS OF A FLAT CHAMPAGNE GLASS COLLECTOR AND A 45°CONICAL COLLECTOR

11.1 Design of the Field Trials

A 5" diameter flat $\alpha = 35°$ champagne glass collector (as in Fig 12a), an $\alpha = 45°$ conical collector and a standard gauge were compared against a reference 5" pit gauge between May 1983 and January 1987 at the Institute of Hydrology, Wallingford. The small diameter of the flat champagne glass was the result of a practical requirement to carry out preliminary field trials using readily available materials. Splash-out is therefore likely to be significant. The rate of rainfall and wind speed were continually monitored by adjacent automatic weather station equipment, so that the measured wind speeds (close to gauge rim height) were averages during rainfall only. The total rainfall and true mean rate of rainfall and mean wind speed in rain were summed over 24-hour periods.

Sevruk's (1982) wetting algorithms have been used to estimate wetting losses for a standard gauge collector including measure and delivery pipe. Wetting losses are a function of rainfall total and, more weakly, climatic conditions at the site. The wetting losses of the 45° conical collector and champagne glass collector alone are estimated to be about half of those of the standard 5" gauge and the pit gauge, which includes a 5" gauge. However the reduced losses are offset (a) by the long (c 25 cm) delivery pipes used for the flat champagne glass and conical gauges and (b) the losses due to the collector bottle and measuring cylinder will be the same

as for the 5" gauges. Table III gives the set of corrections used; seasonal variations have not been included.

TABLE III CORRECTIONS FOR WETTING ERRORS APPLIED TO WALLINGFORD TRIALS RAINFALL DATA (MM) ADAPTED FROM SEVRUK (1982)

DAILY RAINFALL TOTAL	5" STANDARD PIT GAUGE	5" STANDARD GAUGE RIM AT 30 cm	45°CONICAL GAUGE RIM AT 30 cm	FLAT CHAMPAGNE GLASS GAUGE RIM AT 30 cm
< 1 mm	0.11	0.11	0.10	0.10
≧ 1 mm	0.22	0.22	0.20	0.20

11.2 Results

Figs 13a-c show observed losses relative to the catch of a 5" reference pit gauge for the 5" standard, 45° conical and flat champagne glass gauges after correction for estimated wetting losses. Only 563 complete sets of daily measurements (all with rainfall) were available, so Figs 13a-c contain considerable sampling errors.

Each point on the graphs is based on daily data grouped into sets of 15-37 observations according to predefined ranges of the "true" value of $\bar{R}$ (from the pit gauge) and of $\bar{u}_o$. The groupings were designed to include as far as possible similar numbers of observations and to sample as wide a range as possible of mean values of $\bar{R}$. Prominent features of Figs 13a-13c are:

(1) The 5" gauge losses (Fig 13a) are clearly a much stronger function of $\bar{u}_o$ than are the 45° conical gauge or flat champagne glass losses (Figs 13b, 13c). Allowing for sampling error, the 5" gauge losses agree quite well with model (Model I) predictions.

(2) The 45° cone and, even more, the flat champagne glass gauge losses are affected by outsplash. Thus, contrary to the model predictions, the largest flat champagne glass gauge losses occur for the highest values of $\bar{R}$ rather than for the lowest. No clear relationship between losses and $\bar{R}$ exists for the 45° conical gauge.

(3) A weak increase in losses with increasing $\bar{u}_o$ can be discerned for the 45° conical gauge for the two lowest values of $\bar{R}$ (0.4 and 0.85 mm h^{-1}). These losses are markedly less than modelled. At higher values of $\bar{R}$, there is little evidence of a relationship between losses and $\bar{u}_o$. Note that the modelled 45° conical gauge losses cannot be easily compared with the field results because of the non-linear relationship of conical gauge losses with $\bar{u}_o$ (section 9).

(4) The flat champagne glass (α = 35°) losses seem to be almost wholly dominated by outsplash. The only suggestion of a weak increase of loss with increasing $\bar{u}_o$ is at $\bar{R}$ = 0.4 mm h^{-1}. Thus if the gauge was redesigned to eliminate outsplash, the raingauge exposure problem could become fairly unimportant, even at quite high values of $\bar{u}_o$ (excluding snow).

(5) Taking all 563 daily rainfall events together, the rainfall totals (uncorrected for their wetting errors) expressed as a percentage of the reference pit gauge rainfall catch were:- flat champagne glass 97.3%, 5" conical gauge 99.1% and 5" standard gauge

94.7%. Given the insensitivity of its losses to $\bar{u}_o$, this confirms that outsplash from the small diameter flat champagne glass gauge must have been considerably greater than that from the 45° conical gauge.

12. SNOWFALL

The "flat champagne glass" collector would, in principle, collect more snow than a cylindrical gauge. Snow has typical vertical velocities in free air in the range 0.75-1.5 m s^{-1} (Mason 1971) so snowflakes behave (in this respect) rather like raindrops of diameter 0.2-0.4 mm. However snow crystals have a more complicated shape, so their drag coefficients will be different functions of relative air velocity than those given by equations 15a-15d. Reformulation of the numerical model is beyond the scope of this paper but insights may still be gained. The model results were cautiously used to estimate losses of snowfall for an α = 45° gauge as follows. Snowfall was modelled (crudely) in terms of a set of snowflakes falling with the same terminal velocities and drag coefficient as equal numbers of raindrops of 0.2, 0.25, 0.3, 0.35 and 0.4 mm diameter. The "snowflakes" were imagined to contain water volumes in the same proportion as the above raindrops. Values of C were calculated from rainfall loss curves for the 5" gauge and the α = 45° conical gauge like those of Figs 6 and 10. An orifice height of 1.7 m above ground was assumed for comparison with losses of snowfall from shielded cylindrical gauges in several Nordic countries as in Fig 14, taken from Førland and Aune (1986). Fig 14 also shows calculated "snowfall" losses for the cylindrical gauge (curve A) and α = 45°conical gauge (curve B). The clear difference between curves A and B suggests that an inverted conical shape of collector in a practical form could have a much greater collection efficiency in snowfall for $\bar{u}_o > 5$

ms^{-1}. Thus the flat champagne glass collector may have potential for improved observations of snowfall compared to unshielded and perhaps shielded cylindrical gauges if "blow out" can be minimised by (a) using a sufficiently large diameter collector with tall enough sides and (b) heating of the inner collector surface.

Another technique might use two adjacent champagne glass gauges with markedly different values of α and therefore different systematic losses. Their catch ratio would vary with the terminal velocities of the snowflakes. Thus "fine" snow, commonest at temperatures well below freezing, would tend to give a catch ratio further from unity than snow composed of larger flakes. This ratio could be used in conjunction with measurements of $\bar{u}_o$ and temperature to make improved corrections to the snowfall catch.

13. CONCLUSIONS

This paper provides a simplified, quantitative theory of raingauge exposure losses which seems to stand up well when compared with a large body of field evidence. A new raingauge collector in the form of a flat champagne glass has been suggested which is potentially much less susceptible to exposure losses and so will have most value at exposed sites. Limited field tests of a prototype flat champagne glass gauge have supported the soundness of the basic scientific ideas underlying the new collector. It would be desirable to optimise the new design using a combination of wind tunnel tests and physical calculations of the type presented in this paper. This is especially needed for the proposed very large diameter gauge (about 1 m) that might be used on ships with particular advantage. Field trials

are essential, especially to show that the problem of splashout can be adequately solved.

A flat champagne glass gauge with a large diameter may go some way to answer the plea made by the WCRP Workshop on Precipitation Data Requirements (WMO, 1986b, see introduction) for a reference gauge that could be used on ships at sea. In combination with other surface measurements and rainfall estimates from atmospheric general circulation models, a sufficient number of such gauges might be used to calibrate satellite measurements of oceanic rainfall. Pairs of champagne glass gauges, with differing values of α, might be even more valuable.

These ideas could be exploited to make progress with the very difficult problem of routine snowfall measurements on land. A single flat champagne glass gauge (or a pair of such gauges of differing α) may need additional heating to melt the snow as quickly as it falls eg for calibrating real time radar rainfall data. Heating may be essential but it needs careful consideration to minimise the evaporation errors which could negate the advantage of a gauge of high intrinsic collection efficiency.

Finally the results of this paper underline the need for corrections to historical precipitation data where these are used to study climate change systematic changes in exposure errors may be especially important in windy or snowy climates.

ACKNOWLEDGEMENTS

This paper could not have been written without a study of the unique M Sc thesis of A C Robinson. I am indebted to Dr J C Rodda for access to this document, for constant encouragement and support and for making available facilities at the Institute of Hydrology, especially for arranging field trials of a "flat champagne glass" gauge. I am grateful to S W Smith, R Furnell and A Tashman for carrying out these trials. I also wish to thank Dr P R Helliwell and Dr M J Green for access to their valuable unpublished work and to Dr M J Green, Dr W Roach, Mr R Brown and Mr D E Parker for valuable criticisms and suggestions. Finally I thank Mr C V Smith for proposing that I should tackle the problem of raingauge exposure.

LIST OF FIGURES

Fig 6 Calculated percentage of incident rainfall collected from Model I for a wide range of drop sizes and $\bar{u}_o$ = 0.5, 2, 5 and 20 ms^{-1}.

Fig 7a Calculated 5" gauge losses from Model I using Best's family of drop size distributions. The losses are expressed as a percentage of incident rainfall and compared to AM's model of observed losses from Hellman gauges. Most results are for n = 2 and R = 0.1, 0.3, 1, 2, 4 and 10 mm h^{-1}. Restricted results for n = 1.85 and n = 2.25.

Fig 7b As Fig 6a but using Ulbrich's family of drop size distributions for μ = -1, 0, 1 and R = 0.1, 1 and 10 mm h^{-1}.

Fig 7c As Fig 7a but using Model II for n = 2 only.

Fig 8 Relationship between wind speed and catch losses for standard gauges expressed as a percentage of the catch of ground level gauges for 17 stations in UK (given by Rodda and Smith, 1986). Their results are compared to various modelled losses for R=1 mm h^{-1}.

Fig 9a Values of k used in the 45° conical gauge model.

Fig 9b Values of θ used in the 45° conical gauge model.

Fig 10 Contributions of drops of different diameter to calculated losses of rainfall from the 45° conical gauge compared to losses from 5" gauges, $\bar{u}_o$ = 3.0 and 10.0 ms^{-1}.

Fig 11 Modelled percentage of rainfall lost from the 45° conical gauge as a function of $\bar{u}_o$ and R for Best's drop parameters n=2 and n=2.25

Fig 12a Flat champagne glass collector — a first guess minimum size.

Fig 12b Flat champagne glass collector for possible use on a ship's mast head.

Fig 13a Observed 5" gauge losses at Wallingford May 1983-Jan 1987, using a pit gauge as a standard.

Fig 13b Observed 45° conical gauge losses at Wallingford, same period.

Fig 13c Observed flat champagne glass gauge losses at Wallingford, same period.

Fig 14 Calculated losses of snowfall, expressed in terms of water equivalent, from an unshielded cylindrical gauge compared to those from a well designed gauge with α = 45° compared to observed losses from shielded Nordic raingauges. A common orifice height of 1.7 m is assumed, with wind speeds measured at 10 m at open sites.

Plate I 5" standard gauge and pit gauge used in the Wallingford field trials.

APPENDIX I

APPROXIMATE INDEPENDENCE OF RAINFALL LOSSES TO THE FREQUENCY DISTRIBUTIONS OF INCIDENT WIND SPEED AND RATE OF RAINFALL

a. FREQUENCY DISTRIBUTION OF WIND SPEED

Assume that the total loss of true incident rainfall falling over a long period of time at a specific rate R_i is given by a linear function of the wind speed at gauge height (true of AM's results and the physical model results up to 5 m s^{-1})

$$L_{R_i} = a(R_i) [u_1 R_i t_1 + u_2 R_i t_2 + \ldots .] \qquad (A1)$$

$R_i t_1$, $R_i t_2$ etc are the rainfall totals at each wind speed u_j, and t_j are the durations of each wind speed u_j during rain. a is a constant for a given value of R_i.

Multiplying and dividing (A1) by T_i, the total duration of rainfall falling at rate R_i, we obtain:-

$$L_{R_i} = a(R_i) R_i T_i \left[u_1 \frac{t_1}{T_i} + u_2 \frac{t_2}{T_i} \ldots .\right] \qquad (A2)$$

Let $p(u_j)$ be the probability that a wind speed u_j occurs during rain. Over a long enough interval we can write (A2) as:-

$$L_{R_i} = a(R_i) R_i T_i \int_j u_j p(u_j) du_j$$

$$= a(R_i) R_i T_i \bar{u}_{R_i} \qquad (A3)$$

and the fractional loss of rainfall is therefore:-

$$L_{FR_i} = a(R_i)\ \bar{u}_{R_i} \qquad (A4)$$

b. FREQUENCY DISTRIBUTION OF RAINFALL

The total rainfall is the sum of all individual rates of rainfall R_i, multiplied by their durations:-

$$R_T = R_1T_1 + R_2T_2 + \ldots\ldots$$

From (A3) the total loss of rainfall is therefore:-

$$L_{RT} = \sum_i L_{R_i} = a(R_1)R_1T_1\ \bar{u}_{R1} + a(R_2)R_2T_2\bar{u}_{R2} + \ldots. \qquad (A5)$$

Assume that there is no systematic dependence of $\bar{u}_R$ on R_i so that $\bar{u}$ and R_i are uncorrelated, ie $\bar{u}$ is the same for all R_i. This is a reasonable assumption on synoptic meteorological grounds in middle latitude climate except perhaps on some mountains. Then from (A4) we obtain:-

$$L_{RT} = \bar{u} \sum_i a(R_i)\ R_i\ T_i$$

Multiplying and dividing by T, the total time for which it rains:-

$$L_{RT} = \bar{u}T \sum_i a(R_i)\ R_i\ p(R_i) \qquad (A6)$$

where $p(R_i)$ is the probability of rainfall with rate R_i.

It remains to determine the loss function $a(R_i)$. The model results [$\bar{u}_o \leq 5$ m s^{-1}] and AM's results suggest that the following is a good representation:-

$$\frac{a(R_i)}{a(\bar{R}_i)} = \frac{2\bar{R}_i}{\bar{R}_i + R_i} \qquad 0.1 < R_i < 10 \text{ mm h}^{-1} \qquad \text{(A7)}$$

So we may write (A4) as:-

$$L_{RT} = 2\bar{u}\ T\ \bar{R}_i\ a(\bar{R}_i) \sum_i \frac{R_i}{\bar{R}_i + R_i}\ p(R_i)$$

As $p(R_i) \to 0$ we can rewrite the above as an integral equation. Noting that

$$P(R_i) = P\left(\frac{R_i}{R_i + R_i}\right) \quad \text{and writing} = \frac{R_i}{\bar{R}_i + R_i} = x_i \text{ then:-}$$

$$L_{RT} = 2\bar{u}\ T\ \bar{R}_i)\ a(\bar{R}_i) \int_i x_i\ p(x_i)dx_i \qquad \text{(A8)}$$

Let R_i be observed in the range 0 to R_{MAX}. Letting $R_{MAX} \to \infty$ we obtain

$$L_{RT} = a(\bar{R}_i)\ \bar{u}\ T\ \bar{R}_i \qquad \text{(A9a)}$$

and the fractional loss of rainfall is

$$L_{FRT} = a(\bar{R}_i)\ \bar{u} \qquad \text{(A9b)}$$

Brief tests were carried out with a number of contrasting numerically defined rainfall distributions to examine equation (A7) for different relationships between R_i and $p(R_i)$ and for different values of $\bar{R}_i$.

It was found that $\sum_i x_i\ p\ (x_i)$ lay in the range $^1/_3$ to $^2/_3$ even when only a few "events" were simulated (its asymtotic value is 0.5). After simulating 25 rainfall events, each repeated for several widely different rainfall distributions, the above factor seemed to lie within the range 0.4 to 0.6 for reasonable values of R_{MAX}. So equations (A9a) and (A9b) may be a useful

approximation no matter what the shape of $p(R_i)$ when considering say several tens of hours of rainfall or more. Note that there is no restriction that $\bar{R}_i$ should be close to its climatological mean value. As noted in section 6 of the main part of the paper, equation 9b may only be correct to about 10-15%, because equation (A7) is approximate.

REFERENCES

Allerup P. and Madsen H. (1979) Accuracy of point precipitation measurements. Danish Met. Institute, Clim. Pap. 5., 84pp.

Allerup P. and Madsen H. (1980) Accuracy of point precipitation measurements. Nordic Hydrology, 11, 57-70.

Austin P.M. and Geotis S.G. (1980) Precipitation measurements over the ocean. Air-sea Interaction, Eds.- F Dobson, L. Hasse and R. Davis, 523-541. Plenum Pub. Corp., New York.

Battan L.J. (1973) Radar Observation of the Atmosphere. University of Chicago Press, 324pp.

Best A.C. (1950) The size distribution of raindrops. Q.J. Roy. Met.Soc., 76, 16-36.

Bogdanova E.G. (1966) Investigation of precipitation measurement losses due to the wind. (in Russian). Trans. Voyeykov Main Geophys. Obs., 195, 40-62.

Bradley R.S., Diaz H.F., Eischeid J.K., Jones P.D., Kelly P.M. and Goodess C.M. (1987) Precipitation fluctuations over Northern Hemisphere land areas since the mid-19th Century. Science, 237, 171-175.

British Rainfall Organisation. (1864-1900) British Rainfall, Annual Vols.

Eckert E.R.G. and Drake R.M. (1972) Analysis of heat and mass transfer. McGraw-Hill Kogakusha Ltd., Tokyo.

Folland C.K (1986a) A simple numerical model of the loss of rainfall catch from a standard 5" gauge due to wind. Proc. ETH/WMO/IAHS Workshop on Correction of Precipitation Measurements, Zurich, 1-3 April 1985, 221-232. WMO TD No 104.

Folland C.K. (1986b) A simple numerical model of the loss of rainfall due to wind from a conically-shaped collector and a suggested new collector shape. Ibid 233-238.

Førland E.J. and Aune B. (1986) Comparison of Nordic methods for Point Precipitation Correction. Ibid, 239-244.

Golubev, V.S. (1979) Correction of point precipitation measurement (USSR experience). (Mimeograph), WMO, Geneva.

Green M.J. and Helliwell P.R. (1972) The effect of wind on the rainfall catch. Distribution of Precipitation in Mountainous Areas, Geilo Symposium, Norway, 31 July — 5 August 1972, WMO/OMM No 326, Vol. II, 27-46.

Green M.J. and Helliwell P.R. (1975) The effect of wind on the catch of seven conventional raingauge collectors. (Unpublished, available from the library of the Institute of Hydrology, Wallingford.)

Heberden W. (1769) On the different quantities of rain which appear to fall, at different heights, over the same spot of ground. Phil. Trans., 59, 359-362.

Helliwell P.R. and Green M.J. (1974) Raingauge performance studies. Final Report to the NERC. Contract F60/5/2 (Unpublished, available from the library of the Institute of Hydrology, Wallingford.)

Marshall J.S. and Palmer W.M (1948) The distribution of raindrops with size. J. Met. Amer. Met Soc., 5, 165-166.

Mason B.J. (1971) The Physics of Clouds. 2nd Edition. Clarendon Press.

Meteorological Office (1969) Observers Handbook, 3rd Edition. HMSO, London.

Mueller C.C. and Kidder E.H. (1972) Rain gage catch variation due to airflow disturbances around a standard rain gage. Water Resources Res., 8, 1077-1082.

Reynolds G. (1971) Ground-level raingauges in Scotland. Weather, 26, 379-381.

Robinson A.C. (1968) The aerodynamic characteristics of rain gauges. Unpublished MSC thesis, 2 vols. University of Southampton. Available from the library of the Institute of Hydrology, Wallingford.

Robinson A.C. and Rodda J.C. (1969) Rain, wind and the aerodynamic characteristics of rain-gauges. Met. Mag., 98, 113-120.

Rodda J.C. (1968) The rainfall measurement problem. General Assembly of Bern, 25 Sept - 7 Oct 1967. Geochemistry, precipitation, evaporation, soil moisture, hydrometry. Reports and discussions. Publ. No 78, Int. Ass. of Scient. Hydrol., IUGG, Gentbrugge (Belgium), 215-231.

Rodda J.C. (1973) Annotated bibliography on precipitation measurement instruments. Reports on WMO/IHD Projects, Report No 17, 278pp, WMO No 343.

Rodda J.C. and Smith S.W. (1986) The significance of the systematic error in rainfall measurement for assessing wet deposition. Atmos. Env., 20, pp 1059-1064.

Serra L. (1958) Possibilités d'amélioration des mesures de précipitations. U.G.G.I. Ass. Int. Hydrol. Sc., Gen. Ass. Toronto, 1957. Publ. No 43, pp 535-545. Translation available in the National Meteorological Library, Bracknell, UK.

Sevruk B. (1982) Methods of correcting for systematic error in point precipitation measurement for operational use. Operational Hydrology Report No 21, 91pp, WMO No 589.

Sevruk B. (ed) (1986) Correction of Precipitation Measurements. ETH/IAHS/WMO Workshop on the Correction of Precipitation Measurements, Zurich, 1-3 April 1985. WMO/TD No 104.

Sevruk B. and Hamon W.R. (1984) International Comparison of National Precipitation Gauges with a Reference Pit Gauge. WMO Instruments and Observing Methods Report No 17. WMO/TD No 38.

Ulbrich C.W. (1983) Natural variations in the analytical form of the raindrop size distribution. J. Clim. and Appl. Met., 22, 1764-1775.

Verploegh G. (1958) Rainfall measurement aboard the Netherlands Ocean Weather Ships "Cirrus" and "Cumulus". K.N.M.I. Wetenschappelijk Rapport 57-003 (IV-014).

Warnick C.C. (1953) Experiments with windshields for precipitation gages. Trans Amer. Geophys. Union, 34, 379-388.

WMO (1986a) Report of the Fourth Session of the JSC/CCCO Toga Scientific Steering Group, New Delhi, 10-14 Feb 1986. WCP-120.

WMO (1986b) Review of Requirements for area-averaged precipitation data, surface-based and space-based estimation techniques, space and time sampling, accuracy and error; data exchange. Workshop on Precipitation Data Requirements, Boulder, Co, 17-19 Oct 1985. WCP-100.

WMO (1986c) Report of the Workshop on global large-scale precipitation data sets for the World Climate Research Programme, Camp Springs , Maryland, 24-26 July 1985. WCP-111.

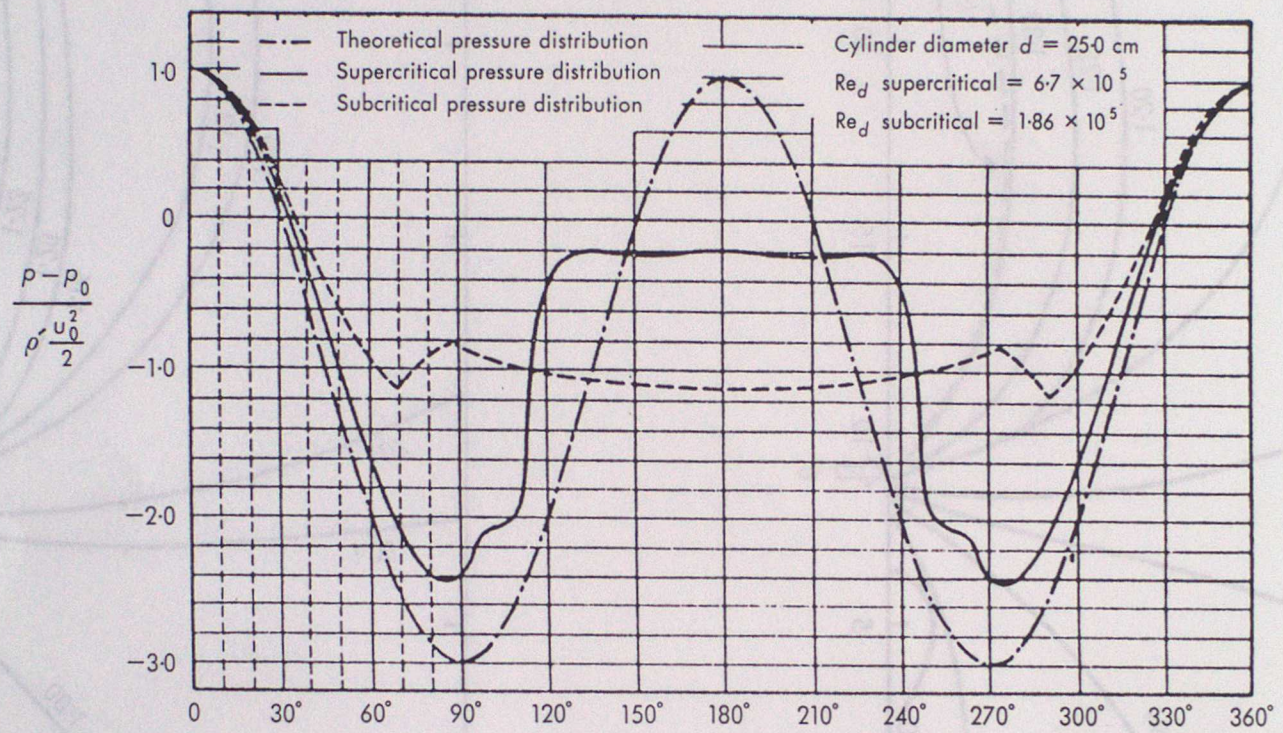
Theoretical pressure distribution
Supercritical pressure distribution
Subcritical pressure distribution
Cylinder diameter d = 25·0 cm
Re_d supercritical = 6·7 × 10^5
Re_d subcritical = 1·86 × 10^5
$\frac{p-p_0}{\rho\frac{u_0^2}{2}}$
1·0
0
−1·0
−2·0
−3·0
0
30°
60°
90°
120°
150°
180°
210°
240°
270°
300°
330°
360°

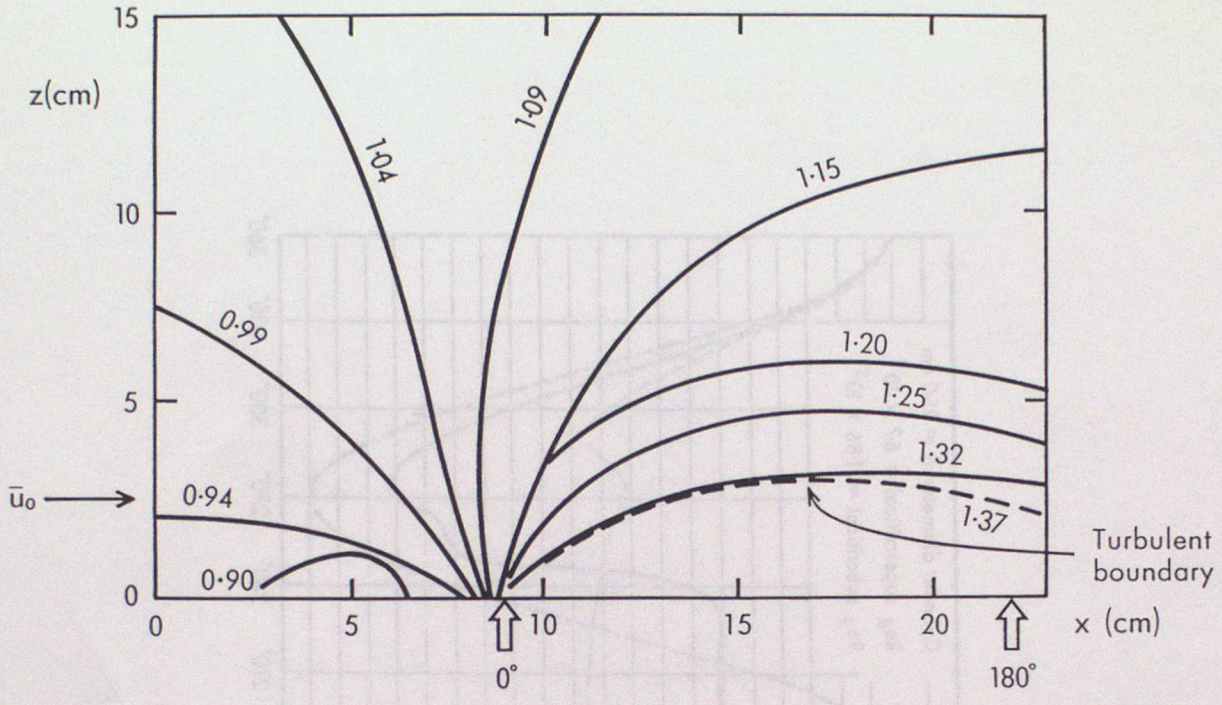
15
z(cm)
10
5
0
$\bar{u}_o$
0
5
10
15
20
x (cm)
0°
180°
1·04
1·09
1·15
0·99
1·20
1·25
1·32
1·37
0·94
0·90
Turbulent
boundary

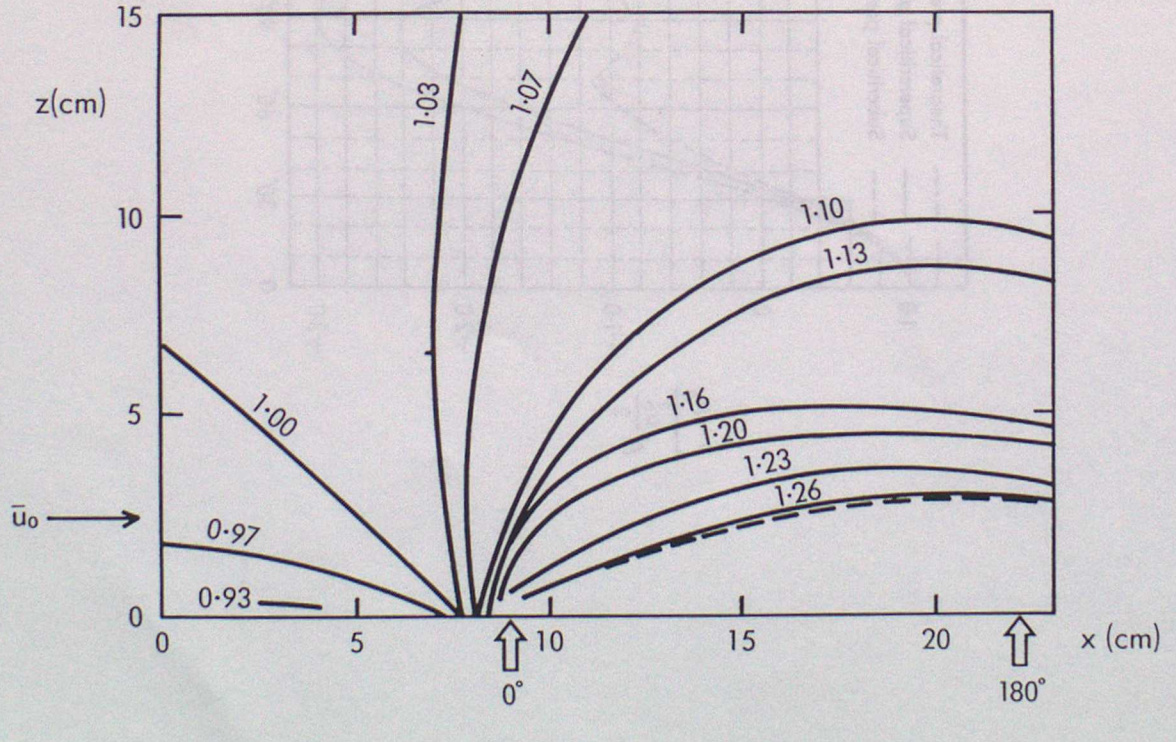
15
z(cm)
10
5
0
$\bar{u}_o$
0
5
10
15
20
x (cm)
0°
180°
1·03
1·07
1·10
1·13
1·00
1·16
1·20
1·23
1·26
0·97
0·93

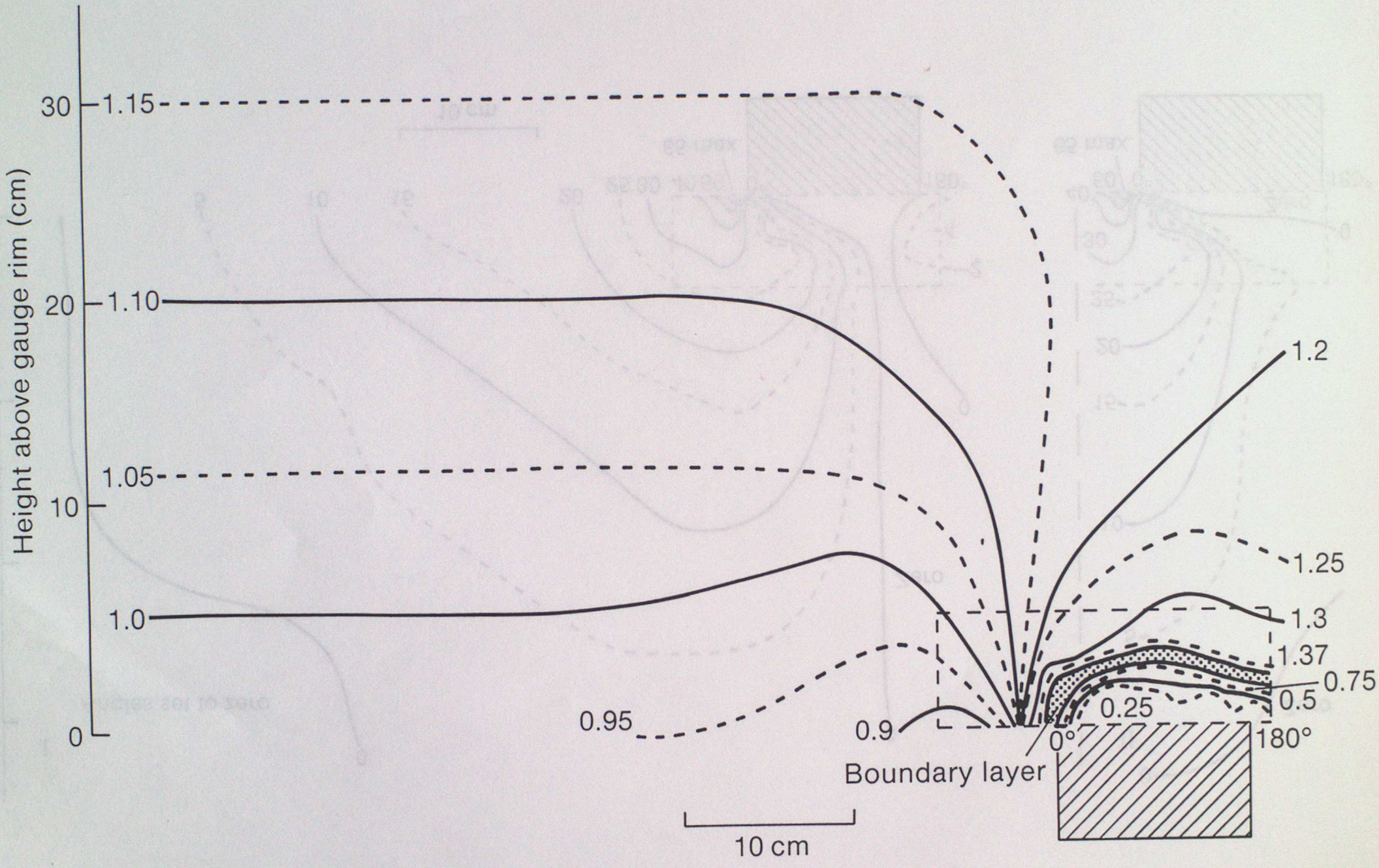
Height above gauge rim (cm)
30
20
10
0
1.15
1.10
1.05
1.0
0.95
0.9
1.2
1.25
1.3
1.37
0.75
0.5
0.25
0°
180°
Boundary layer
10 cm

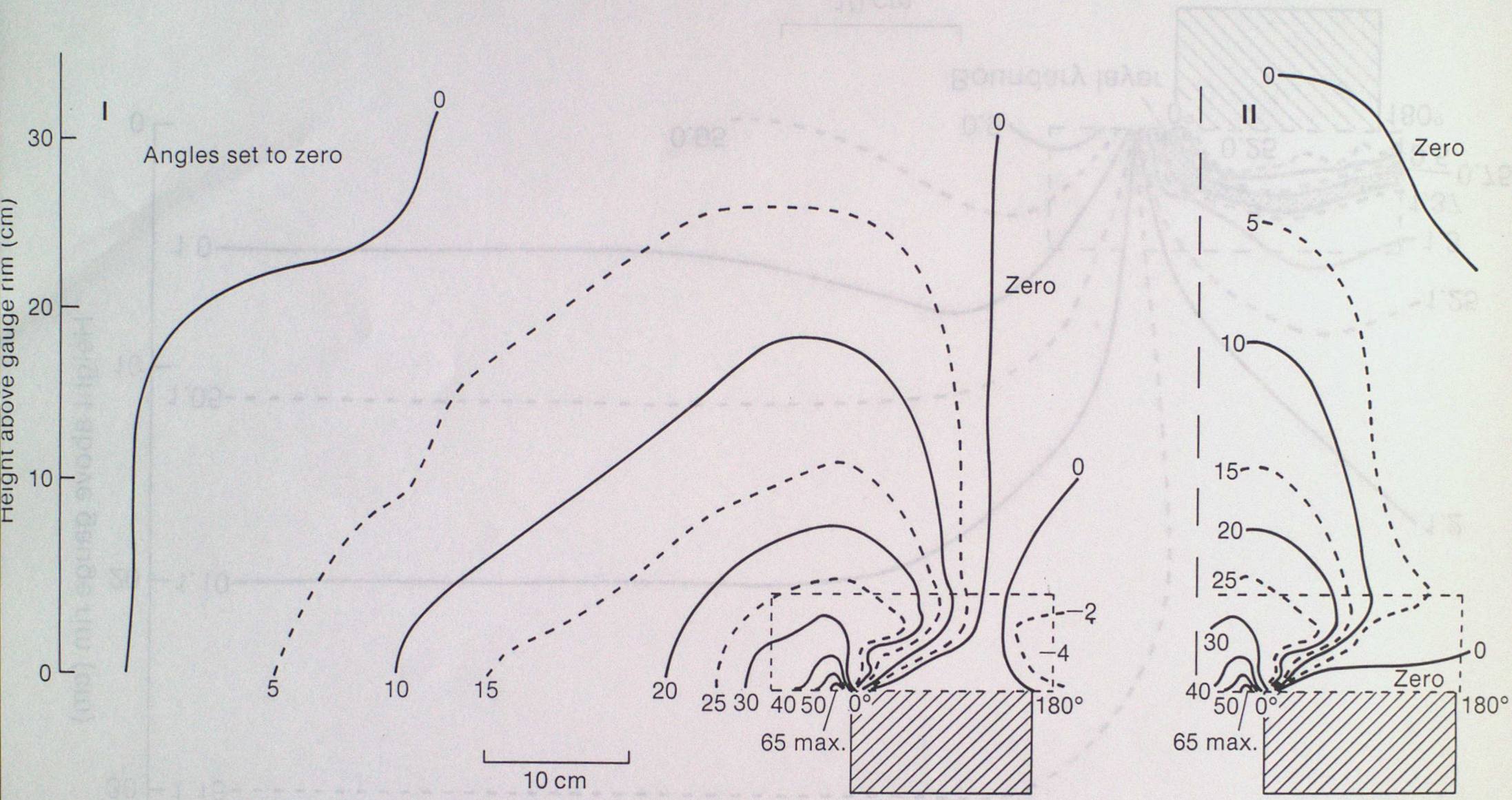
Height above gauge rim (cm)
30
20
10
0
I
Angles set to zero
0
5
10
15
20
25 30
40 50
65 max.
0°
180°
Zero
0
−2
−4
10 cm
II
Zero
5
10
15
20
25
30
40
50
65 max.
0°
180°
0
Zero

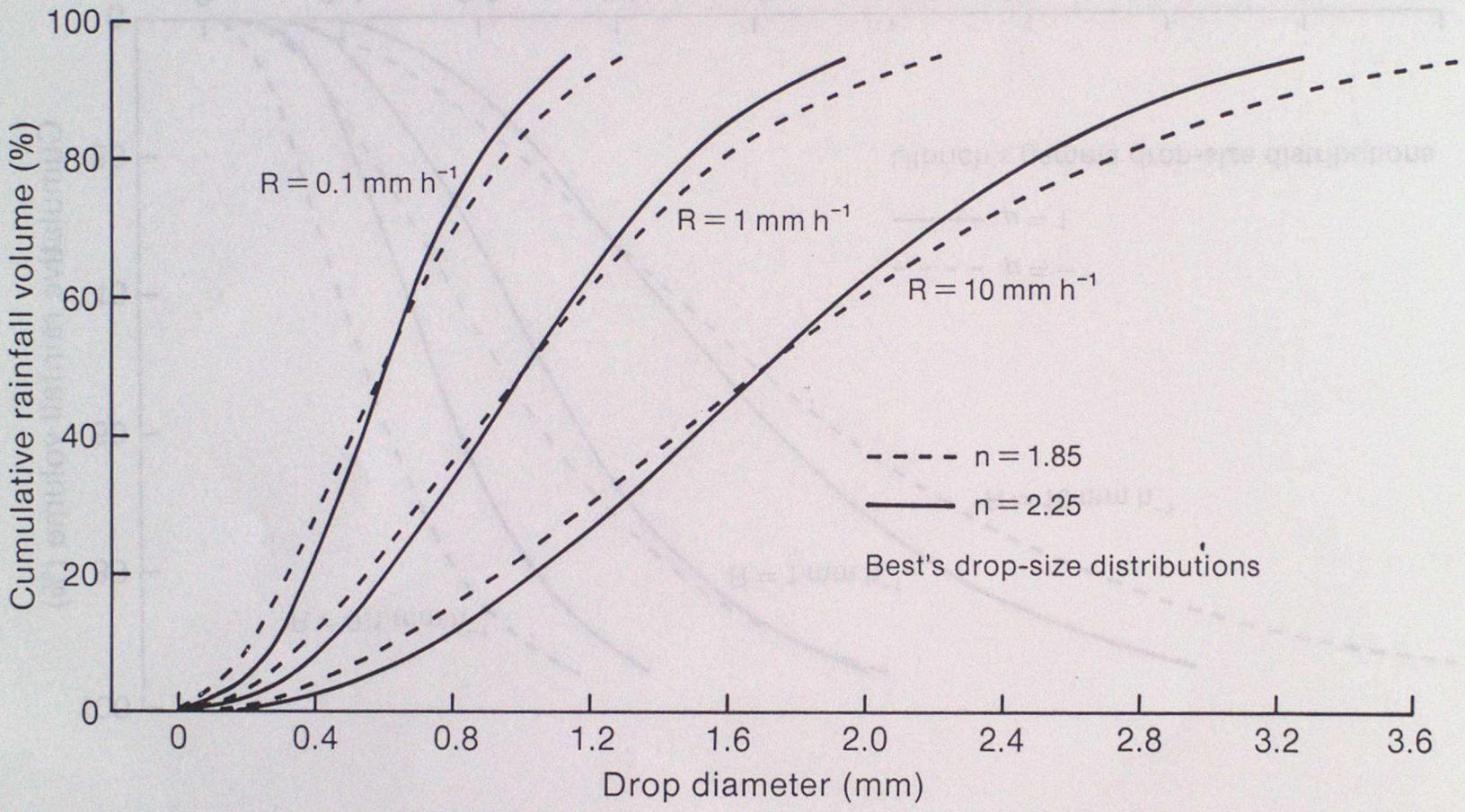
100
80
60
40
20
0
Cumulative rainfall volume (%)
R = 0.1 mm h⁻¹
R = 1 mm h⁻¹
R = 10 mm h⁻¹
n = 1.85
n = 2.25
Best's drop-size distributions
0
0.4
0.8
1.2
1.6
2.0
2.4
2.8
3.2
3.6
Drop diameter (mm)

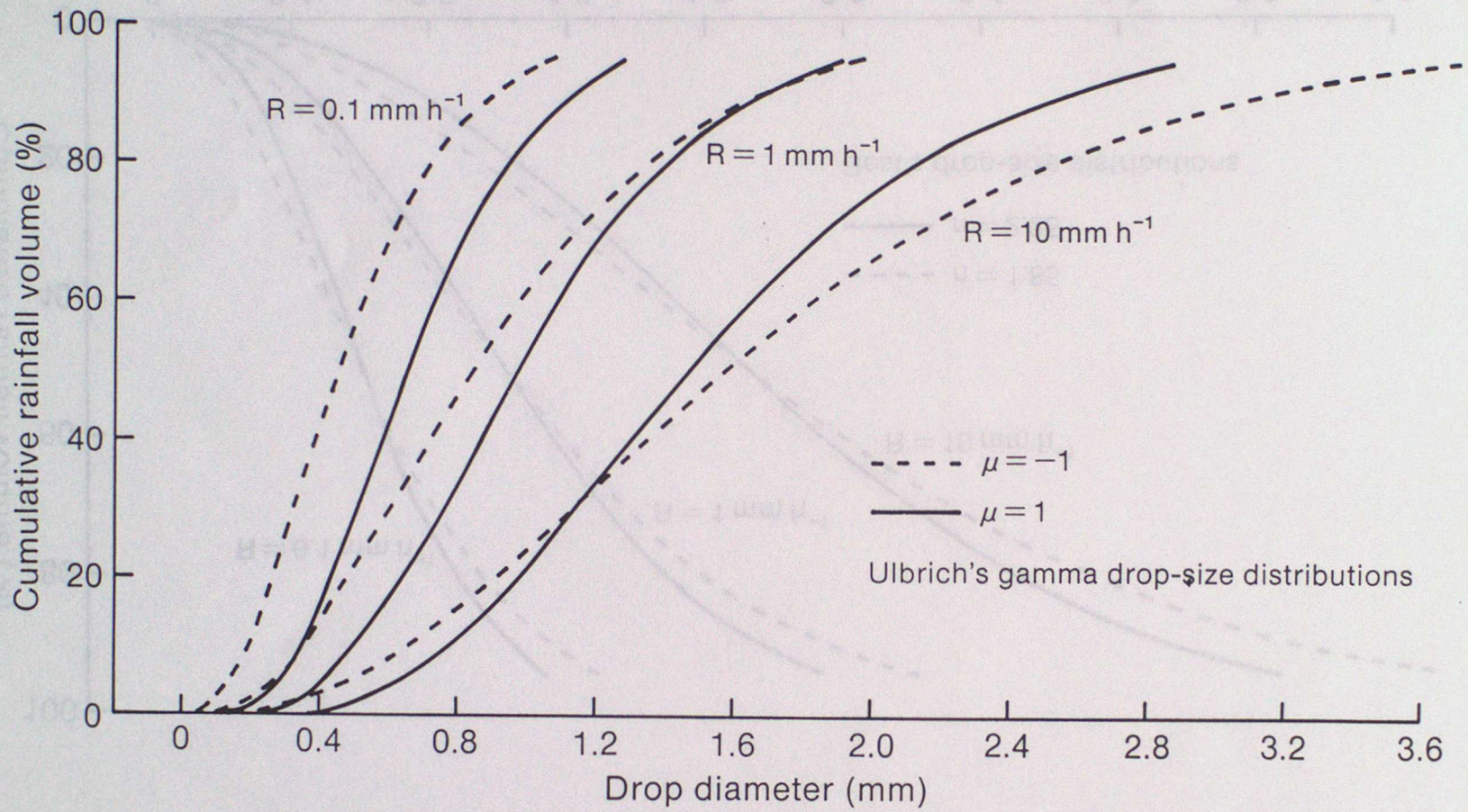
100
80
60
40
20
0
Cumulative rainfall volume (%)
R = 0.1 mm h⁻¹
R = 1 mm h⁻¹
R = 10 mm h⁻¹
μ = −1
μ = 1
Ulbrich's gamma drop-size distributions
0
0.4
0.8
1.2
1.6
2.0
2.4
2.8
3.2
3.6
Drop diameter (mm)

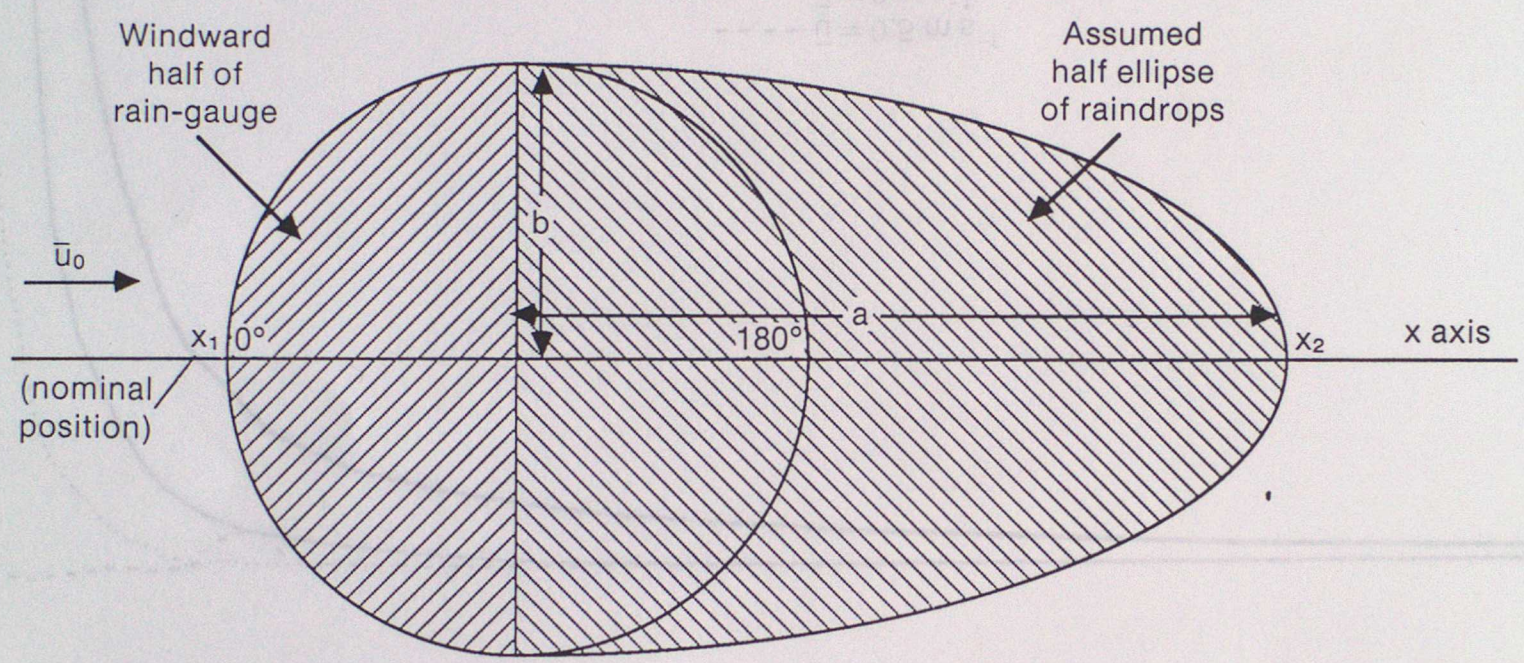
Windward
half of
rain-gauge
Assumed
half ellipse
of raindrops
$\bar{u}_0$
b
a
x_1
0°
180°
x_2
x axis
(nominal
position)

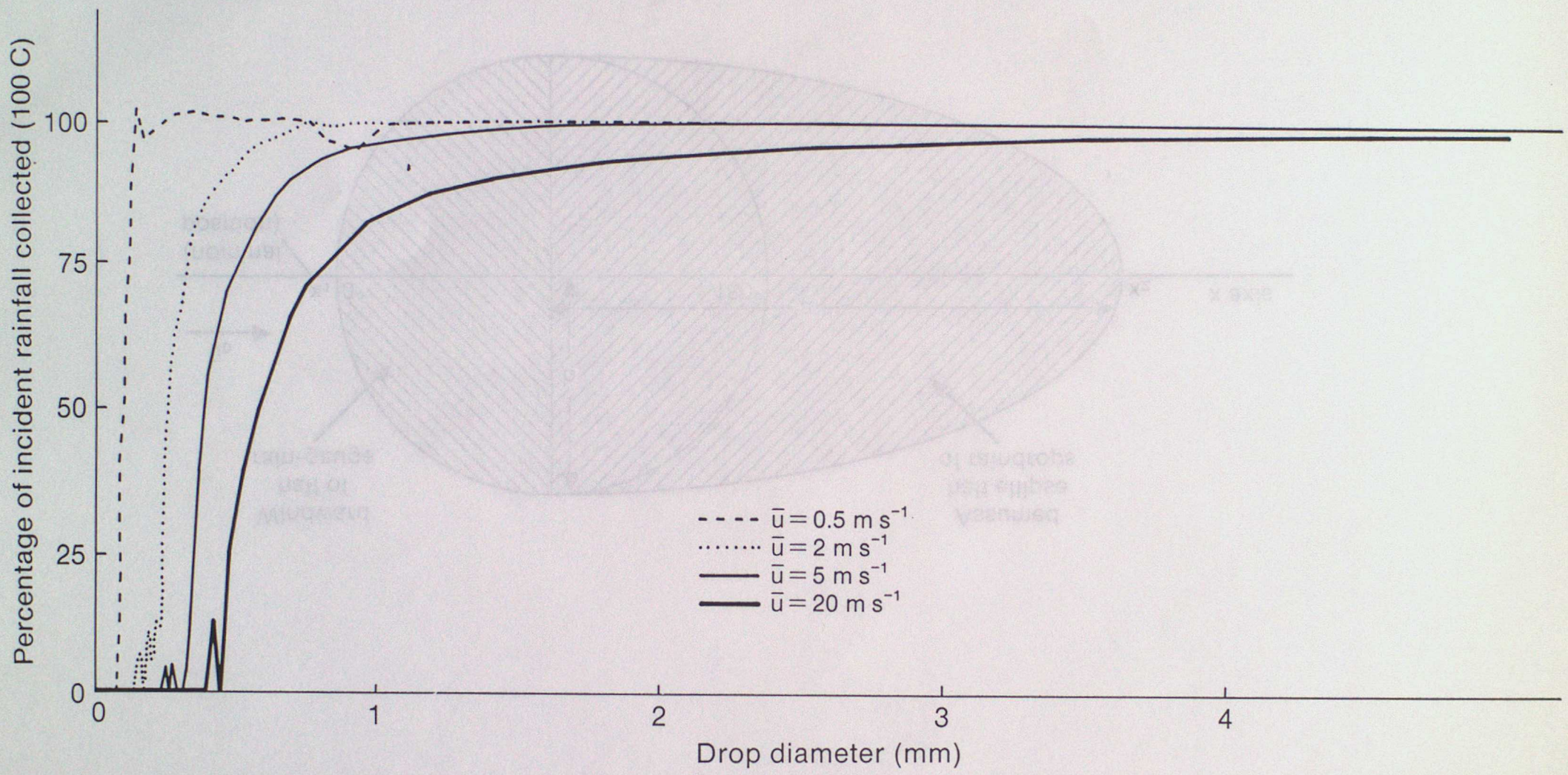
Percentage of incident rainfall collected (100 C)
100
75
50
25
0
0
1
2
3
4
Drop diameter (mm)
$\bar{u} = 0.5\ m\ s^{-1}$
$\bar{u} = 2\ m\ s^{-1}$
$\bar{u} = 5\ m\ s^{-1}$
$\bar{u} = 20\ m\ s^{-1}$

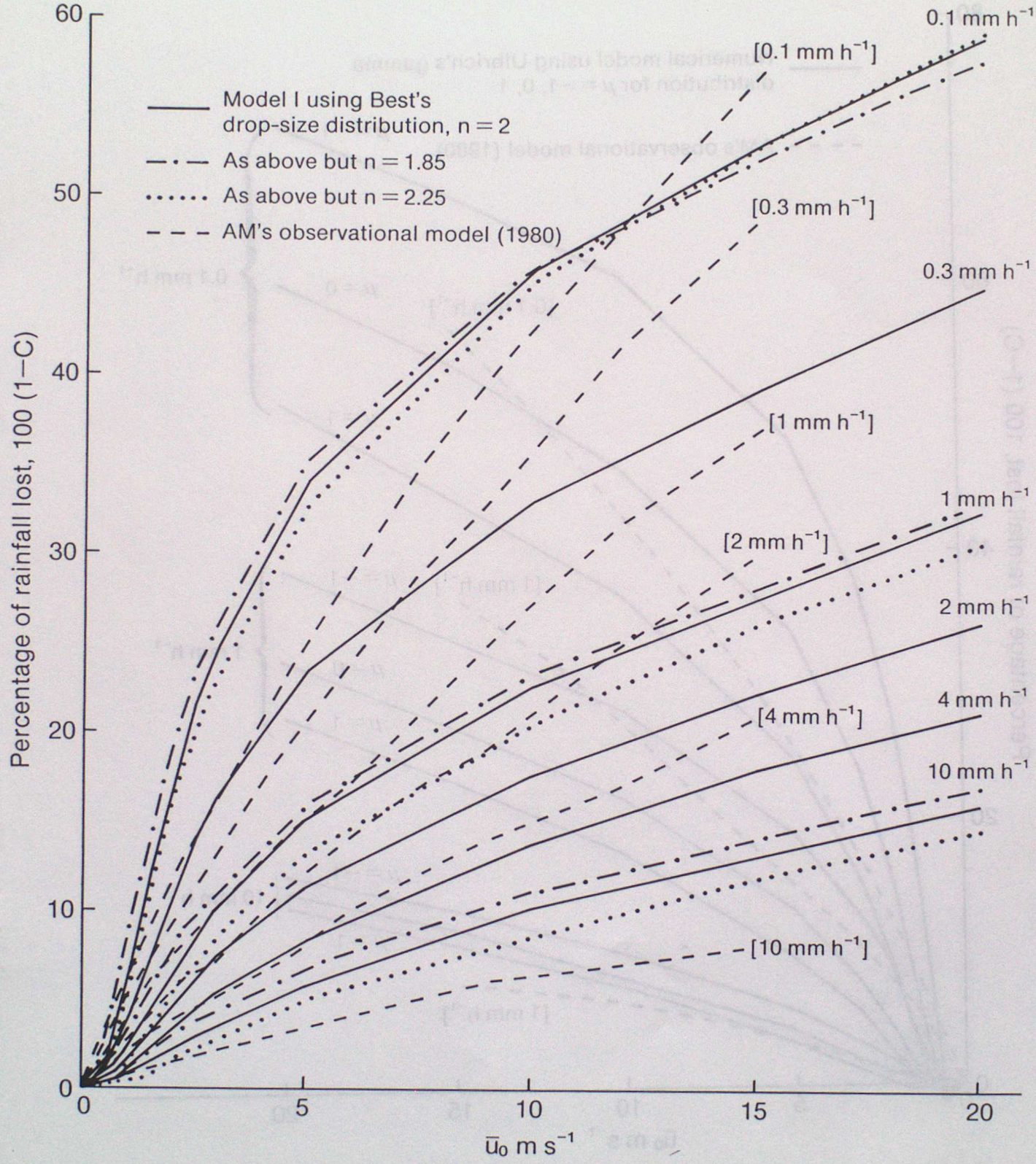
Model I using Best's drop-size distribution, n = 2
As above but n = 1.85
As above but n = 2.25
AM's observational model (1980)
0.1 mm h⁻¹
[0.1 mm h⁻¹]
[0.3 mm h⁻¹]
0.3 mm h⁻¹
[1 mm h⁻¹]
1 mm h⁻¹
[2 mm h⁻¹]
2 mm h⁻¹
4 mm h⁻¹
[4 mm h⁻¹]
10 mm h⁻¹
[10 mm h⁻¹]
Percentage of rainfall lost, 100 (1−C)
0
10
20
30
40
50
60
0
5
10
15
20
ū₀ m s⁻¹

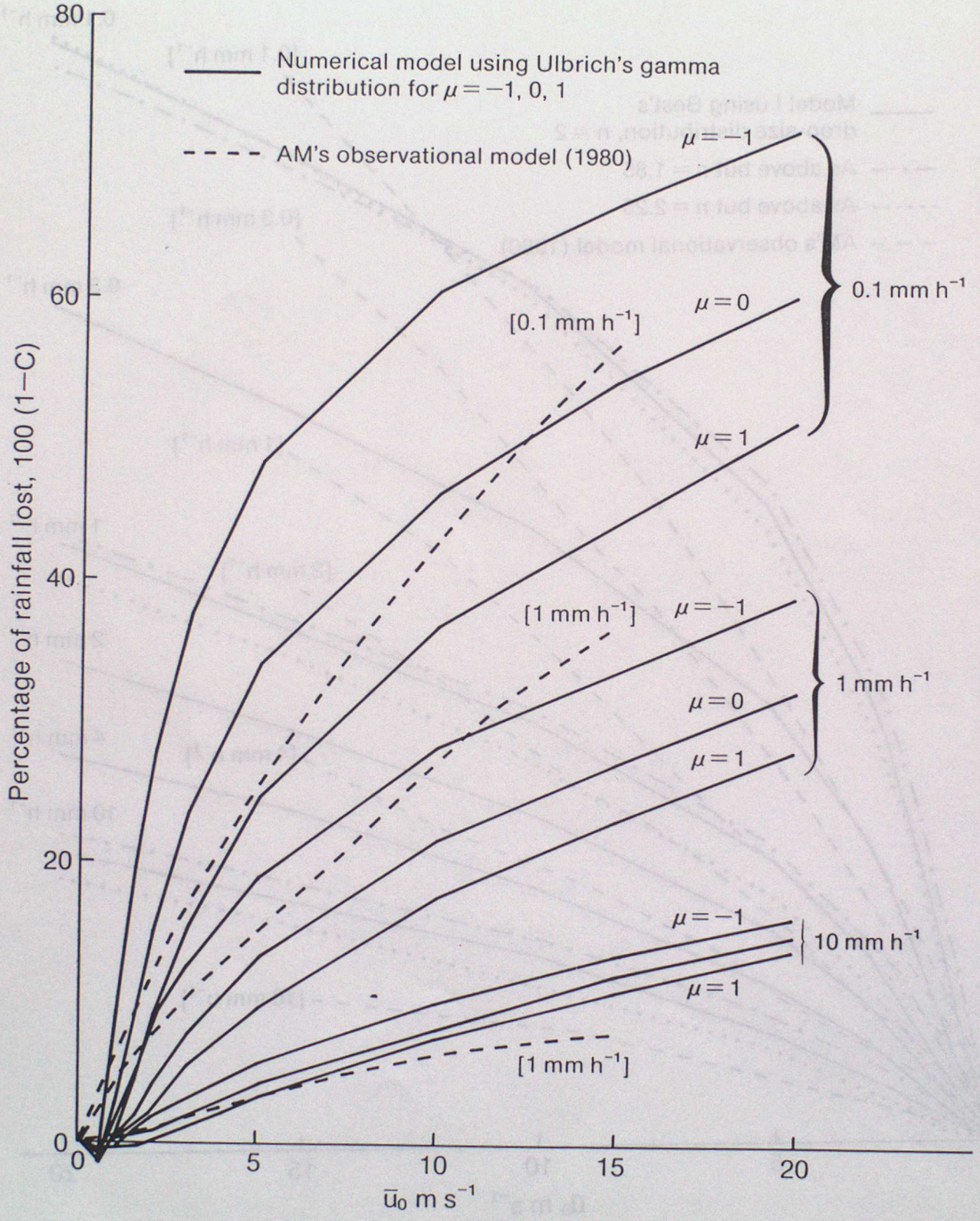
Numerical model using Ulbrich's gamma distribution for $\mu = -1, 0, 1$
AM's observational model (1980)
$\mu = -1$
$\mu = 0$
$\mu = 1$
0.1 mm h^{-1}
[0.1 mm h^{-1}]
[1 mm h^{-1}]
1 mm h^{-1}
10 mm h^{-1}
Percentage of rainfall lost, 100 (1−C)
$\bar{u}_0$ m s^{-1}
0
20
40
60
80
5
10
15
20

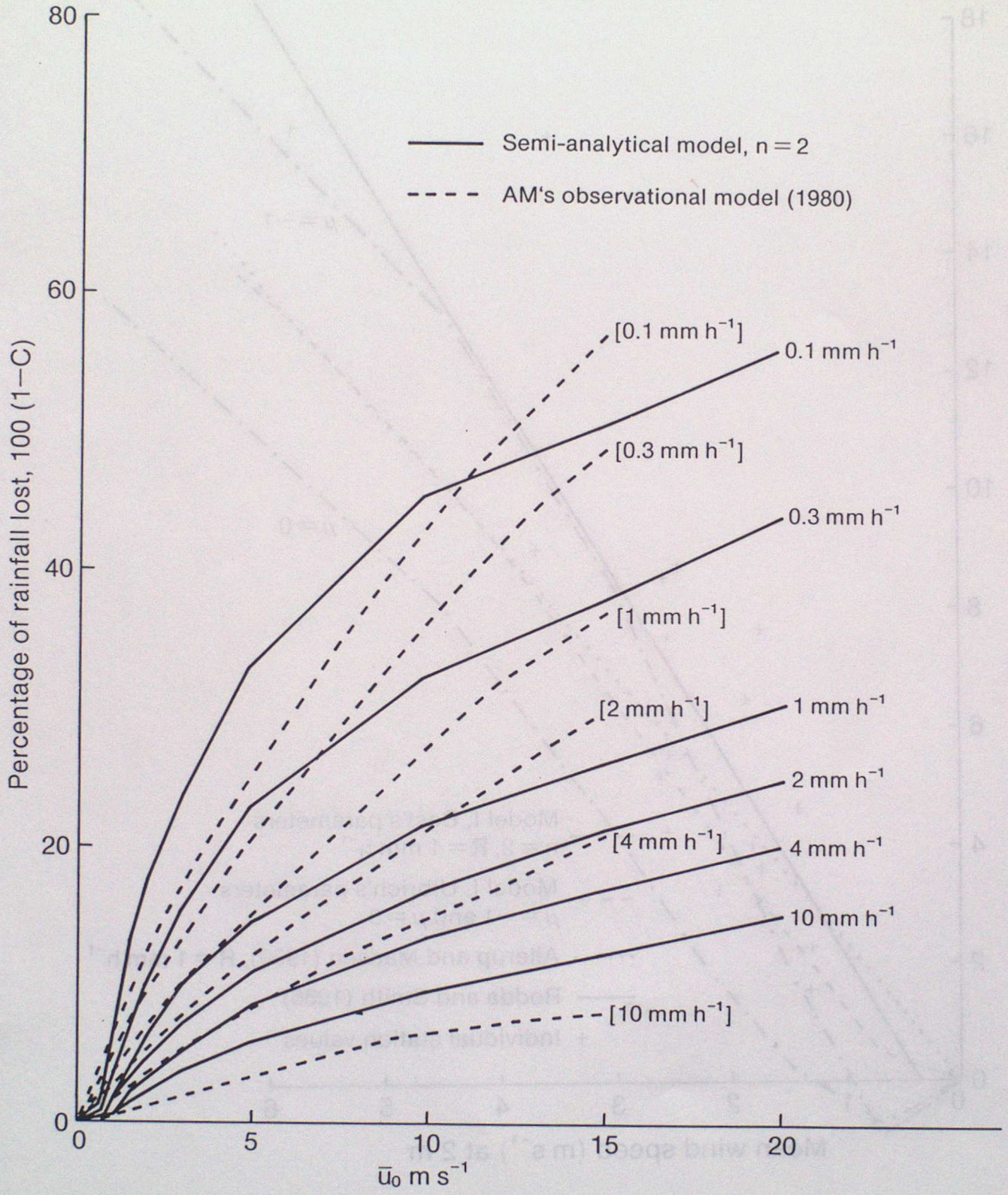
Semi-analytical model, n = 2
AM's observational model (1980)
Percentage of rainfall lost, 100 (1−C)
80
60
40
20
0
0
5
10
15
20
$\bar{u}_0$ m s^{-1}
[0.1 mm h^{-1}]
0.1 mm h^{-1}
[0.3 mm h^{-1}]
0.3 mm h^{-1}
[1 mm h^{-1}]
[2 mm h^{-1}]
1 mm h^{-1}
2 mm h^{-1}
[4 mm h^{-1}]
4 mm h^{-1}
10 mm h^{-1}
[10 mm h^{-1}]

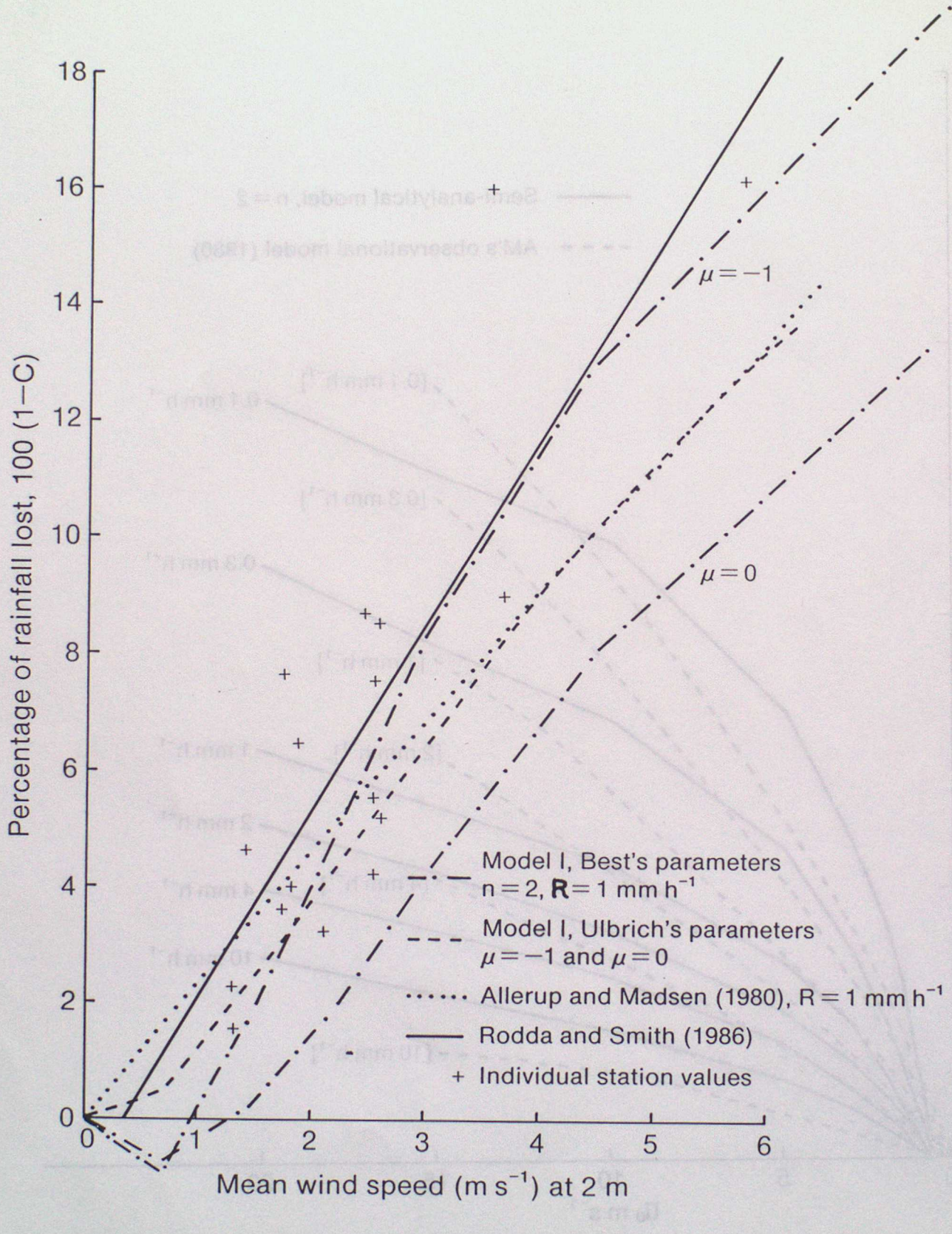
Percentage of rainfall lost, 100 (1−C)
18
16
14
12
10
8
6
4
2
0
0
1
2
3
4
5
6
Mean wind speed (m s⁻¹) at 2 m
μ = −1
μ = 0
Model I, Best's parameters
n = 2, R = 1 mm h⁻¹
Model I, Ulbrich's parameters
μ = −1 and μ = 0
Allerup and Madsen (1980), R = 1 mm h⁻¹
Rodda and Smith (1986)
Individual station values

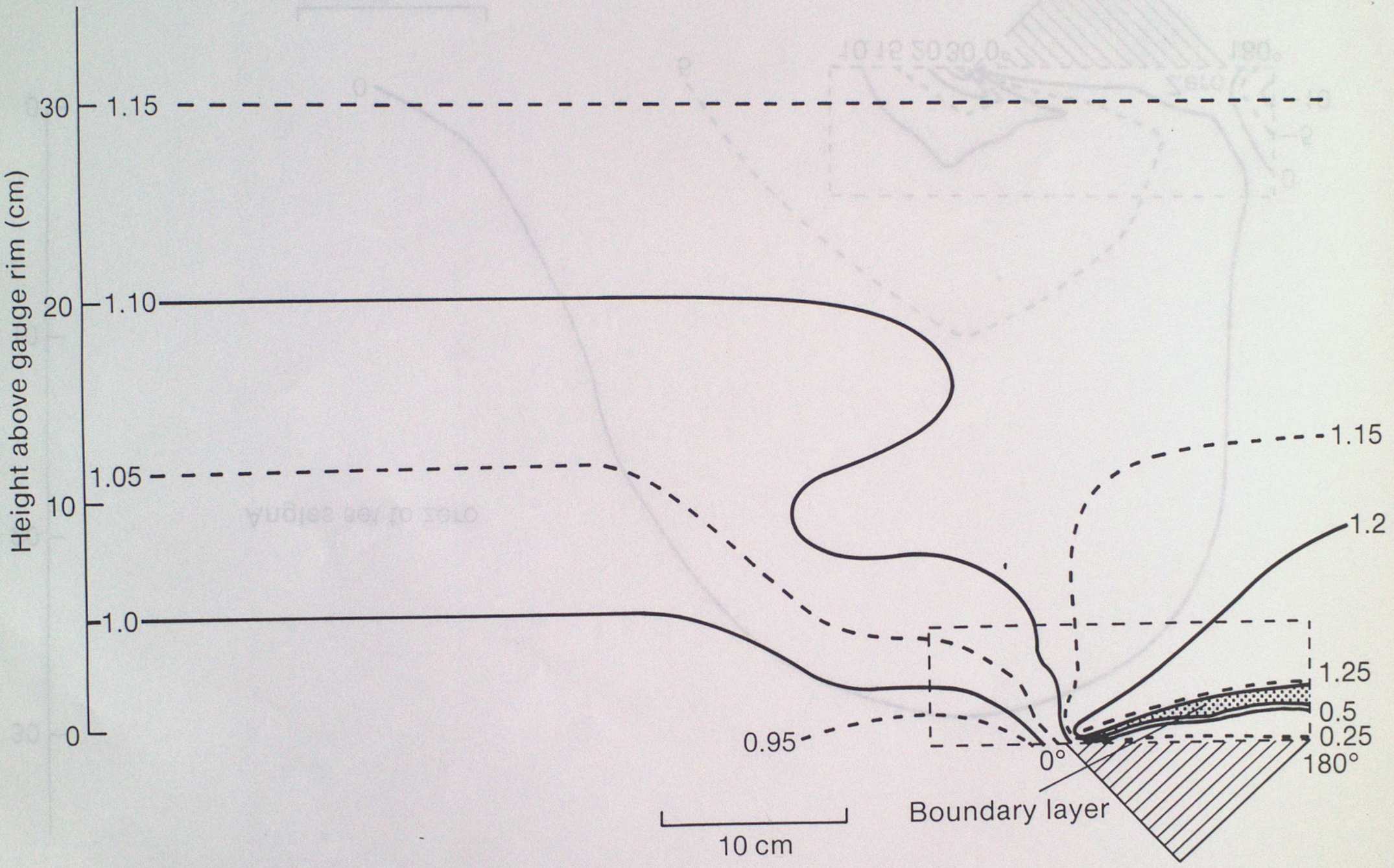
Height above gauge rim (cm)
30
20
10
0
1.15
1.10
1.05
1.0
0.95
1.15
1.2
1.25
0.5
0.25
0°
180°
Boundary layer
10 cm

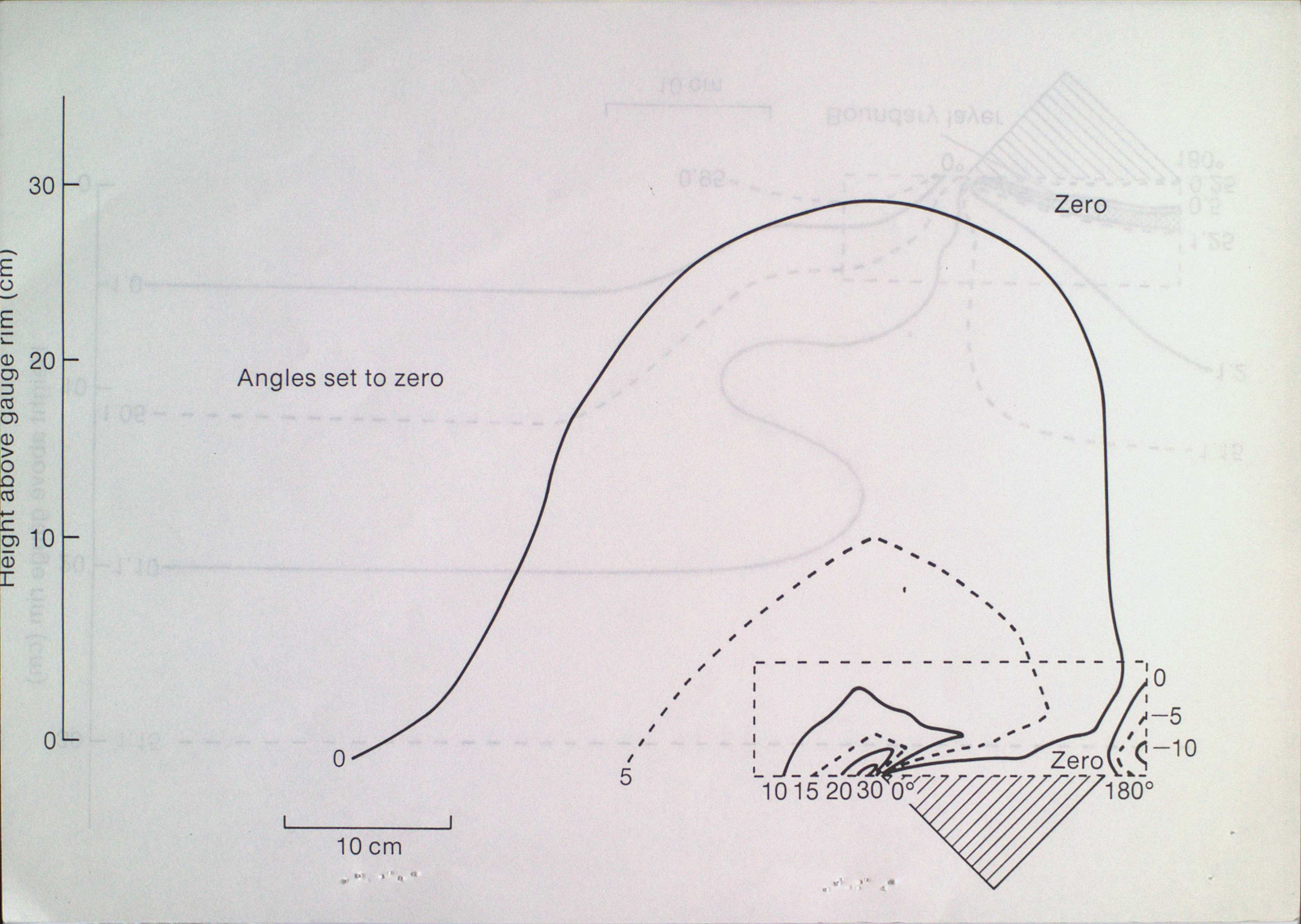
Height above gauge rim (cm)
30
20
10
0
Angles set to zero
Zero
0
10 cm
5
0
−5
−10
Zero
10 15 20 30 0°
180°

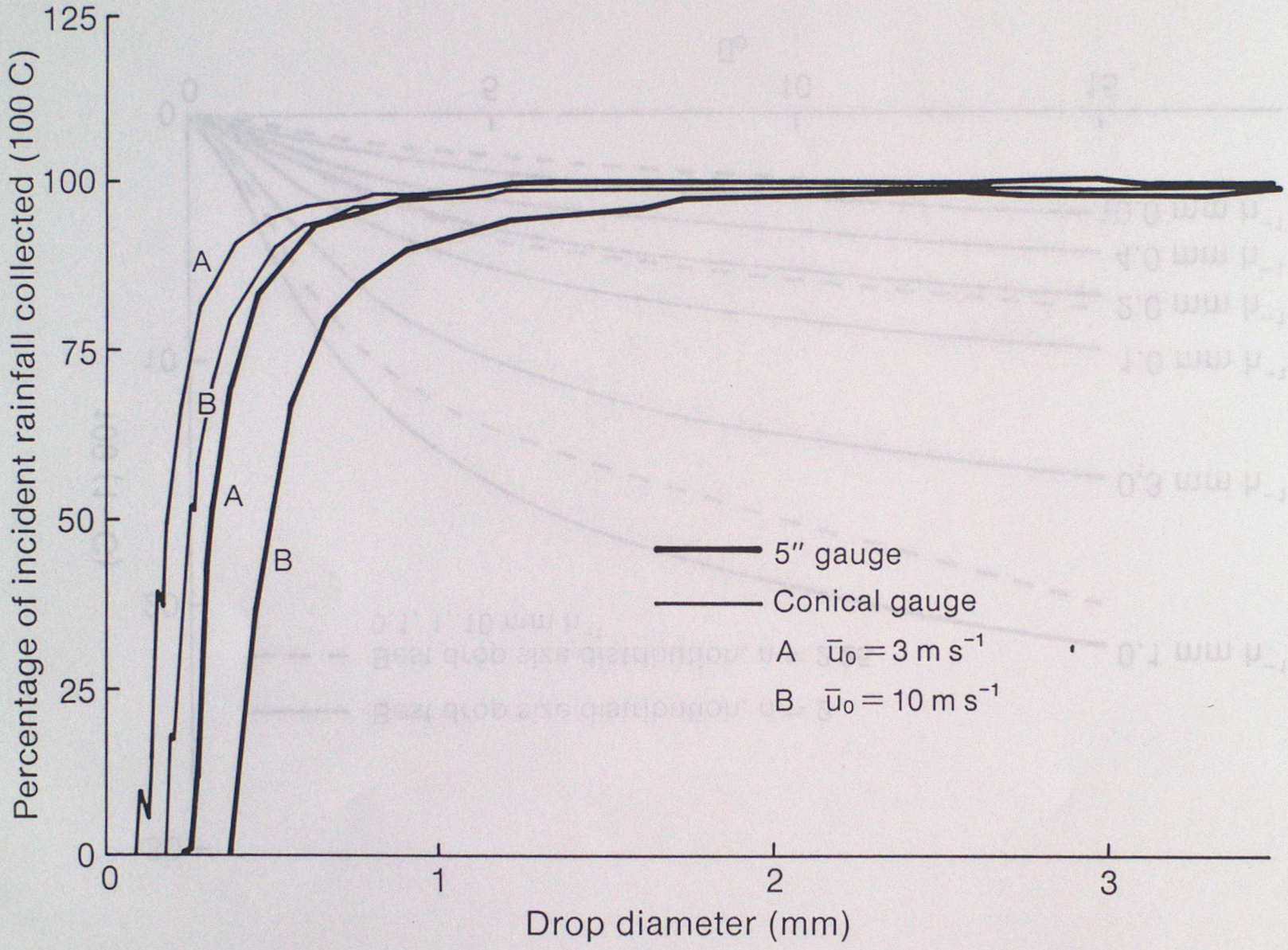
Percentage of incident rainfall collected (100 C)
125
100
75
50
25
0
0
1
2
3
Drop diameter (mm)
A
B
A
B
5″ gauge
Conical gauge
A $\bar{u}_0 = 3\ m\ s^{-1}$
B $\bar{u}_0 = 10\ m\ s^{-1}$

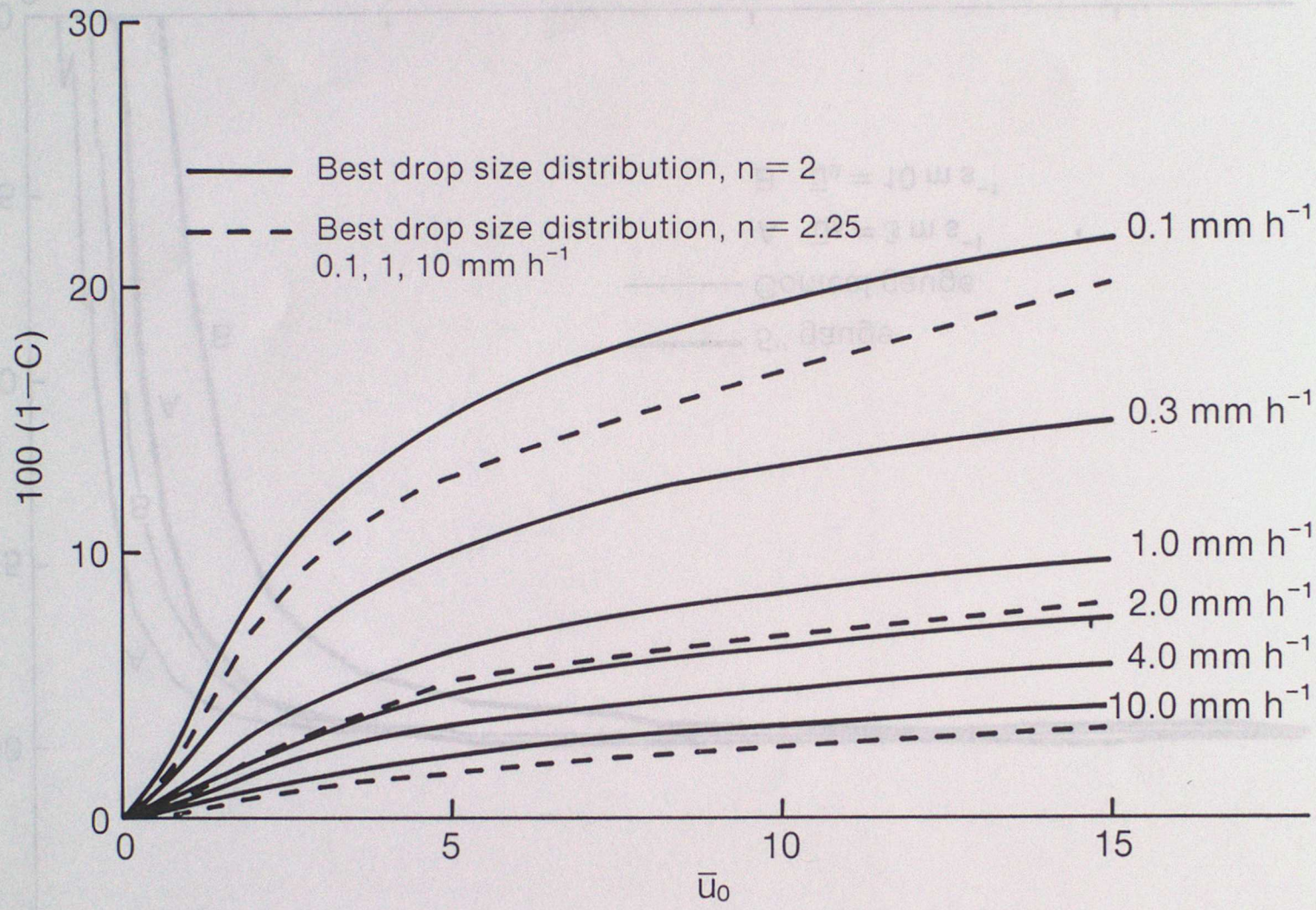
30
20
10
0
100 (1−C)
Best drop size distribution, n = 2
Best drop size distribution, n = 2.25
0.1, 1, 10 mm h^{-1}
0.1 mm h^{-1}
0.3 mm h^{-1}
1.0 mm h^{-1}
2.0 mm h^{-1}
4.0 mm h^{-1}
10.0 mm h^{-1}
0
5
10
15
$\bar{u}_0$

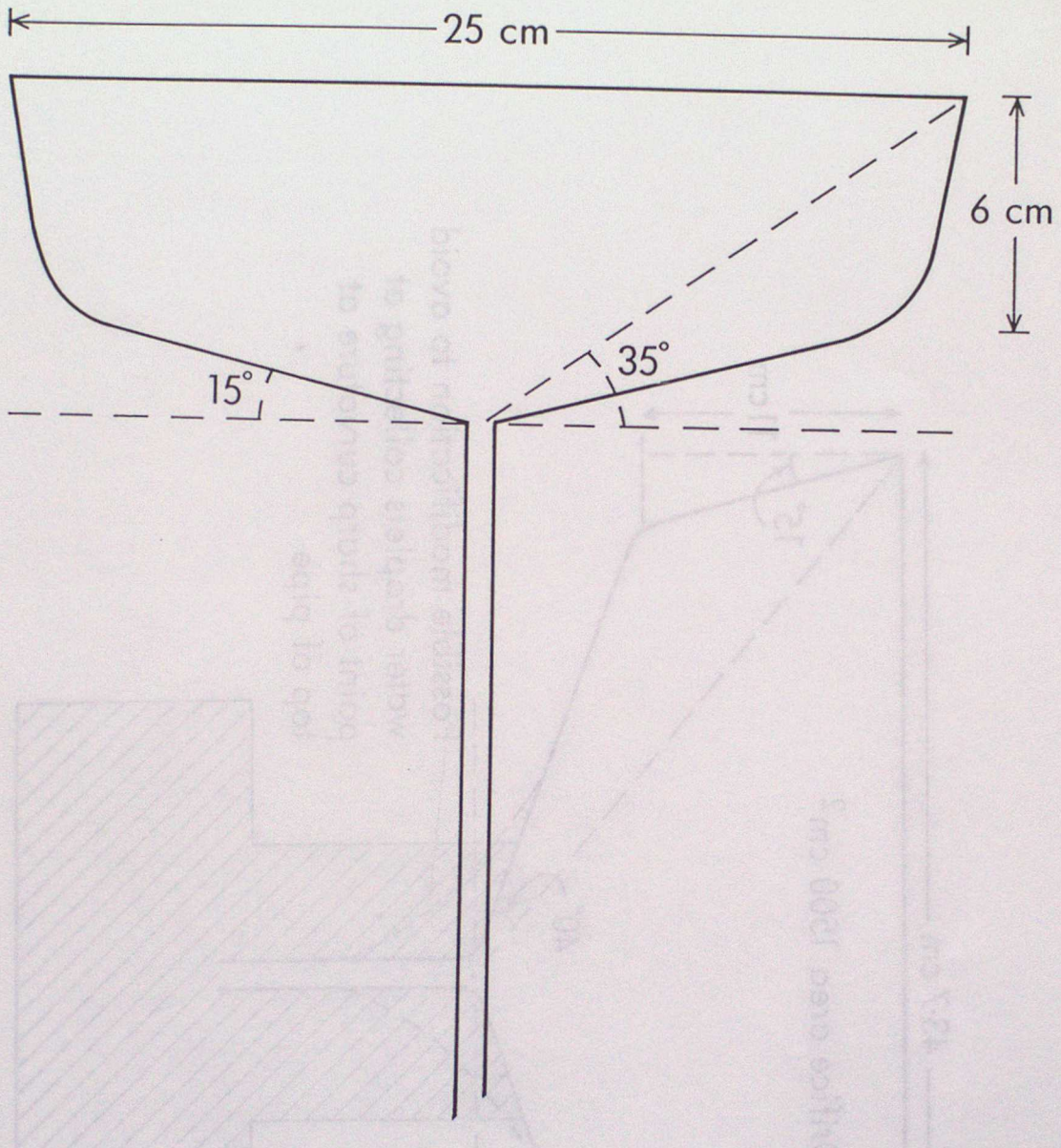
25 cm
6 cm
15°
35°

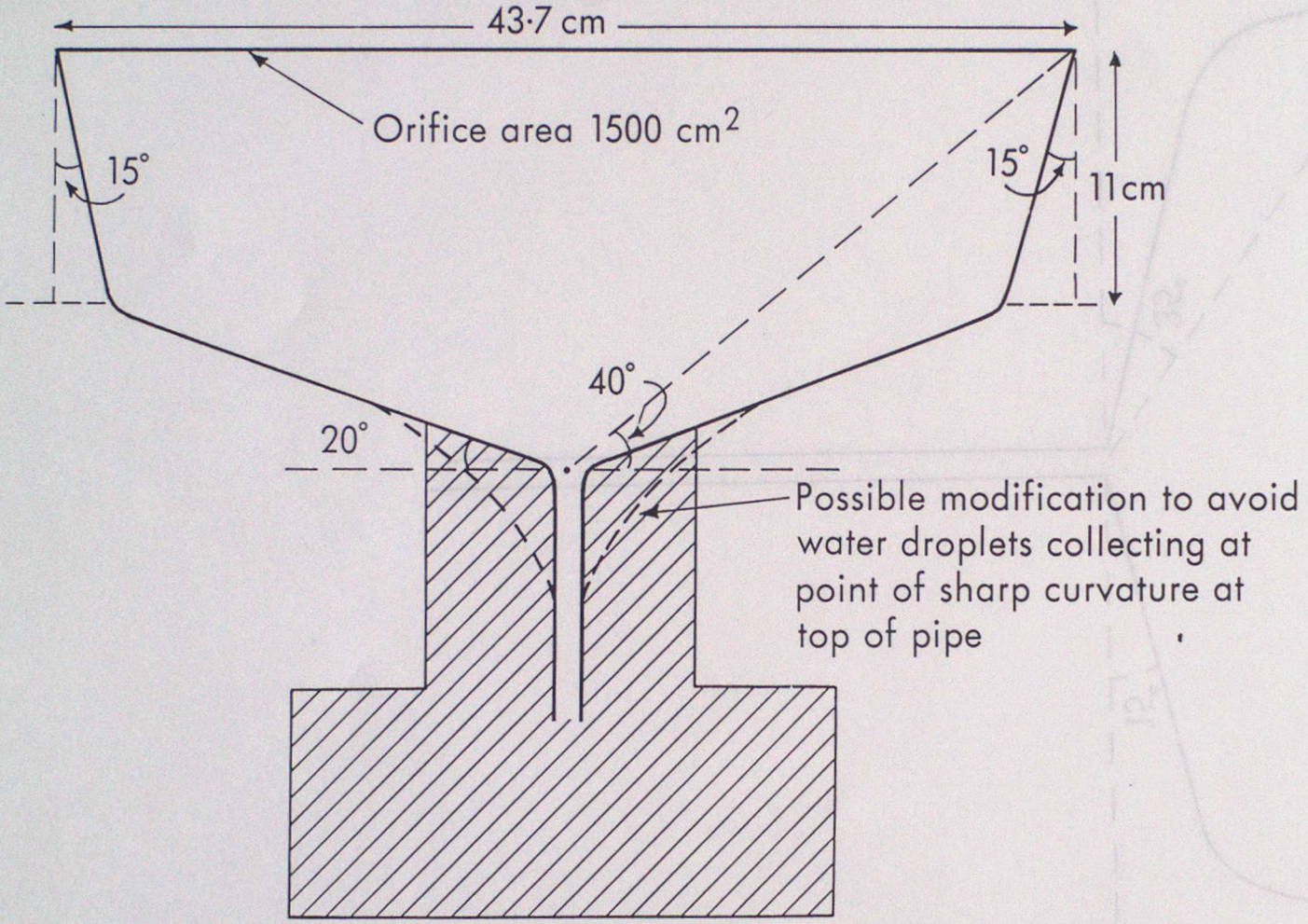
43·7 cm
Orifice area 1500 cm²
15°
15°
11 cm
40°
20°
Possible modification to avoid water droplets collecting at point of sharp curvature at top of pipe

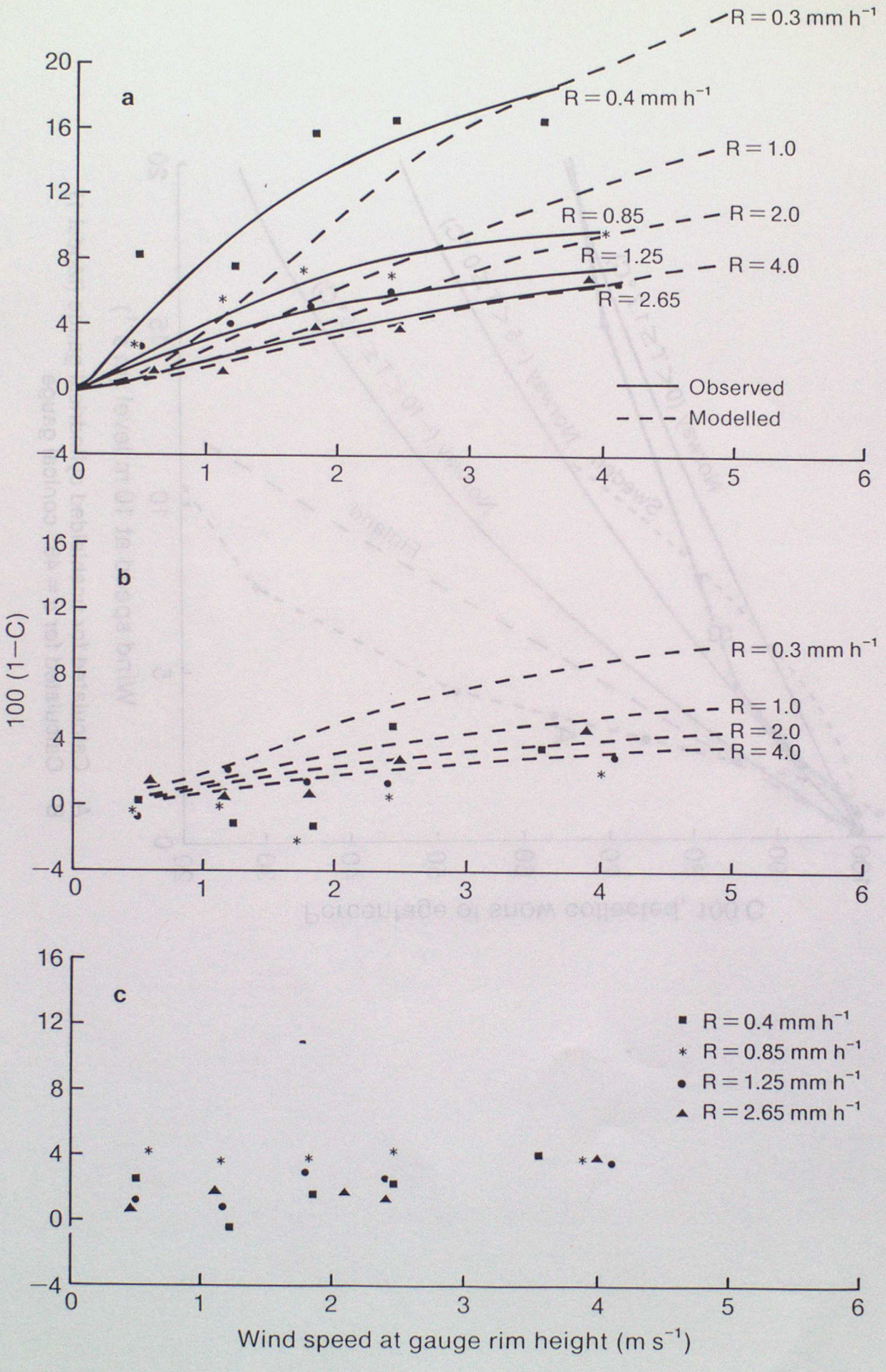
a
b
c
R = 0.3 mm h⁻¹
R = 0.4 mm h⁻¹
R = 1.0
R = 0.85
R = 2.0
R = 1.25
R = 4.0
R = 2.65
Observed
Modelled
100 (1−C)
R = 0.4 mm h⁻¹
R = 0.85 mm h⁻¹
R = 1.25 mm h⁻¹
R = 2.65 mm h⁻¹
Wind speed at gauge rim height (m s⁻¹)

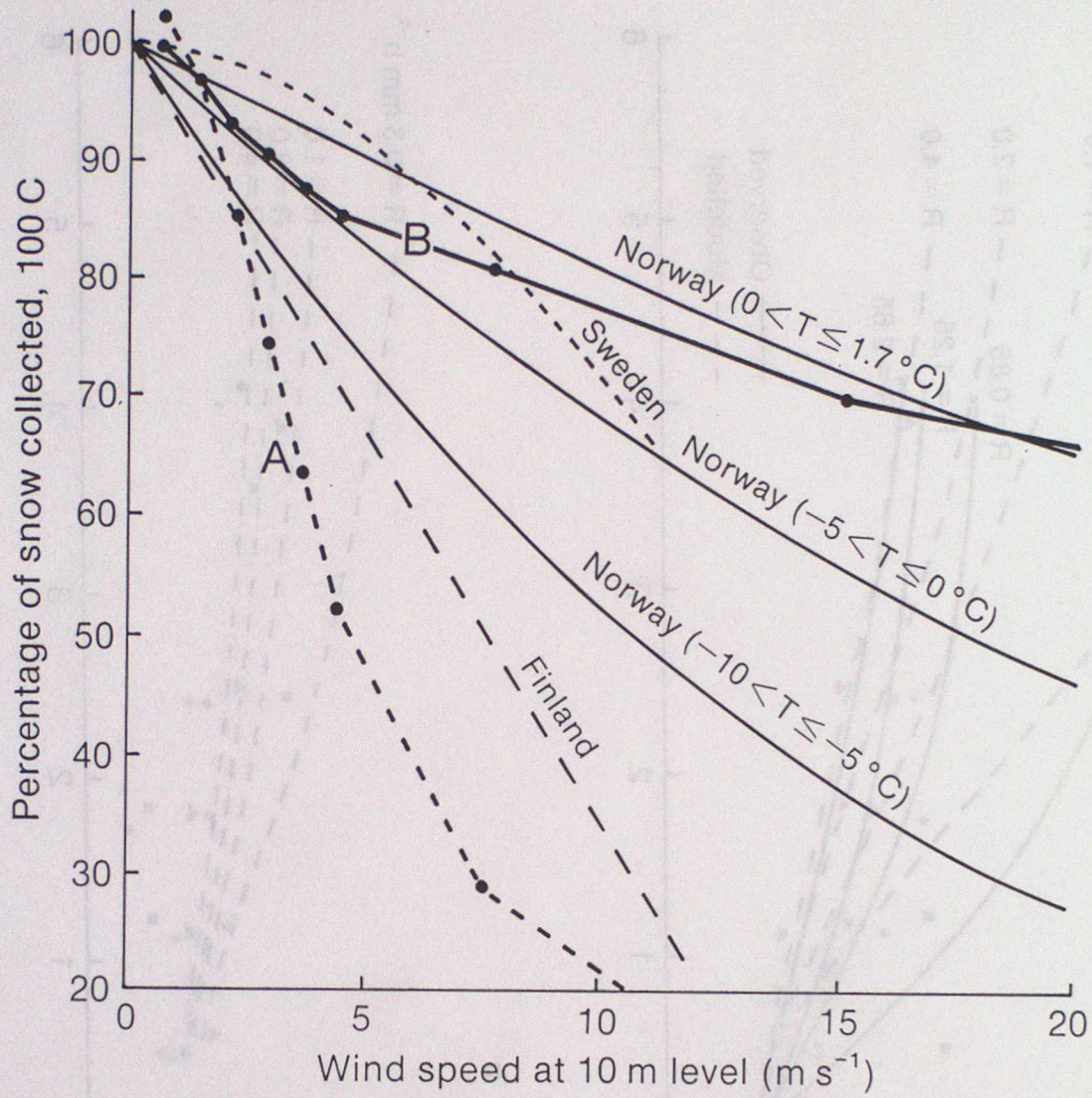

A Calculated for unshielded cylindrical gauge (Model 1)
B Calculated for $\alpha = 45°$ conical gauge

INDEX TO LONG-RANGE FORECASTING AND CLIMATE RESEARCH SERIES

1) THE CLIMATE OF THE WORLD - Introduction and description of world climate.
by C K Folland (March 1986)

2) THE CLIMATE OF THE WORLD - Forcing and feedback processess.
by C K Folland (March 1986)

3) THE CLIMATE OF THE WORLD - El Nino/Southern Oscillation and the Quasi-biennial Oscillation.
by C K Folland (March 1986)

4) THE CLIMATE OF THE WORLD - Climate change: the ancient earth to the 'Little Ice Age'.
by C K Folland

5) THE CLIMATE OF THE WORLD - Climate change: the instumental period.
by C K Folland (March 1986)

6) THE CLIMATE OF THE WORLD - Carbon dioxide and climate (with appendix on simple climate models).
by C K Folland (March 1986)

7a) Sahel rainfall, Northern Hempishere circulation anomalies and worldwide sea temperature changes, (To be published in the Proceedings of the "Pontifical Academy of Sciences Study Week", Vatican, 23-27 September 1986).
by C K Folland, D E Parker, M N Ward and A W Colman (September 1986)
(Amended July 1987)

8) Lagged-average forecast experiments with a 5-level general circulation model.
by J M Murphy (March 1986)

9) Statistical Aspects of Ensemble Forecasts.
by J M Murphy (July 1986)

10) The impact of El Nino on an Ensemble of Extended-Range Forecasts.
(Submitted to Monthly Weather Review)
by J A Owen and T N Palmer (December 1986)

11) An experimental forecast of the 1987 rainfall in the Northern Nordeste region of Brazil.
by M N Ward, S Brooks and C K Folland (March 1987)

12) The sensitivity of Estimates of Trends of Global and Hemispheric Marine Temperature to Limitations in Geographical Coverage.
by D E Parker (April 1987)

13) General circulation model simulations using cloud distributions from the GAPOD satellite data archive and other sources.
by R Swinbank (May 1987)

14) Similation of the Madden and Julian Oscillation in GCM Experiments.
by R Swinbank (May 1987)

15) Numerical simulation of seasonal Sahel rainfall in four past years using observed sea surface temperatures.
by J A Owen, C K Folland and M Bottomley
(April 1988)

16) Not used

17) A note on the use of Voluntary Observing Fleet Data to estimate air-sea fluxes.
by D E Parker (April 1988)

18) Extended-range prediction experiments using an 11-level GCM
by J M Murphy and A Dickinson (April 1988)

19) Numerical models of the Raingauge Exposure problems - field experiments and an improved collector design.
by C K Folland (May 1988)

20) An interim analysis of the leading covariance eigenvectors of worldwide sea surface temperature anomalies for 1901-80.
by C K Folland and A Colman (April 1988)